Green Metrics and Sustainability in Photocatalysis

Green Metrics and Sustainability in Photocatalysis

Arianna Quintavalla,*[a],[b] Davide Carboni,[a] and Marco Lombardo*[a],[b]

[a] Prof. A. Quintavalla, Dr. D. Carboni, Prof. M. Lombardo
Department of Chemistry “G. Ciamician”
Center for Chemical Catalysis - C3
Alma Mater Studiorum, University of Bologna
Via P. Gobetti 85, 40129 Bologna, Italy
E-mail: arianna.quintavalla@unibo.it, marco.lombardo@unibo.it
[b] Prof. A. Quintavalla, Prof. M. Lombardo
Consorzio C.I.N.M.P.I.S. (National Interuniversity Research Consortium in Innovative Synthesis Methodologies and Processes)
c/o Alma Mater Studiorum - University of Bologna
Via P. Gobetti 85, 40129 Bologna, Italy

Abstract: In the past century, significant advancements in synthetic chemistry undeniably contributed to the wellness of mankind, from the development of new drugs to the design of materials for energy production and storage. However, this technological progress has also brought forth significant challenges, emphasizing the urgent need to rethink chemistry for more environmentally friendly approaches. In this Review a critical and comprehensive analysis of the sustainability in the preparation of commonly used photocatalysts is performed, by employing mass-based metrics. Additionally, a comparative evaluation is made between some selected photocatalytic protocols and traditional reactions not relying on light. The objective is to quantitatively evaluate claims of sustainability and greenness commonly associated with photocatalysis, by exploring the real impact of photocatalytic procedures on waste generation. This quantitative approach provides insights into the broader concept of sustainable processes, challenging assumptions and encouraging a more rigorous evaluation of green claims in catalysis. Furthermore, the toxicity of the involved species and the availability of the required chemical elements is commented on to provide a global perspective on the sustainability of the analyzed transformations. The results shed light on the true environmental footprint of photocatalysis and reveal that the notion of green chemistry can sometimes be overstated.

1. Introduction

In mid-2008, MacMillan and Nicewicz disclosed the first enantioselective α-alkylation of aldehydes by combining asymmetric organocatalysis with visible light photoredox catalysis, exploiting the well-known $Ru(bpy)_3^{2+}$ complex both as one-electron photo-oxidant and as one-electron reductant (Scheme 1a, bpy = 2,2’-bipyridine).[1] Remarkably, less than one month later that same year, Yoon and co-workers proposed an efficient [2+2] enone radical cycloaddition, triggered by the same visible light photocatalyst (Scheme 1b).[2] Finally, in early 2009, Stephenson and co-workers reported the use of $Ru(bpy)_3^{2+}$ in tin-free reductive dehalogenation reactions under visible light (Scheme 1c).[3] These three seminal papers marked the renaissance of visible light photoredox catalysis as a powerful tool in synthetic organic chemistry and paved the way for the tremendous number of discoveries made in the last fifteen years using visible light to promote novel organic transformations under mild conditions.[4]

Over a century ago, Giacomo Ciamician already envisioned a future world where sunlight-driven photochemical transformations would fuel a more sustainable chemical industry,[5] and still today, photoredox catalytic processes are considered an efficient and greener alternative for the more sustainable construction of molecular architectures.[6] Recently, Reiser, König and co-workers critically compared classical and photocatalytic processes for a selected class of important chemical transformations, qualitatively highlighting their advantages and limitations.[7] The fundamental idea behind this concept is that photons used in visible light photocatalysis are traceless and, therefore, inherently sustainable reagents, capable of providing the energy required to foster a chemical transformation or to activate catalytic intermediates under mild conditions and without producing any waste. While this notion holds generally true, often photocatalytic processes are conducted in the presence of more than stoichiometric sacrificial chemicals, using large excesses of reagents, toxic solvents or specifically designed starting materials. It is now well-established that the assessment of the sustainability of a chemical transformation is a complex issue that cannot be easily resolved by focusing on a single factor. Ideally, life cycle assessment (LCA) should be used to accurately evaluate the sustainability of a chemical process. However, this approach is often only feasible at an industrial scale, due to the extensive data requirements and lengthy timeframes, which are not compatible with the demands of process optimization.[8]

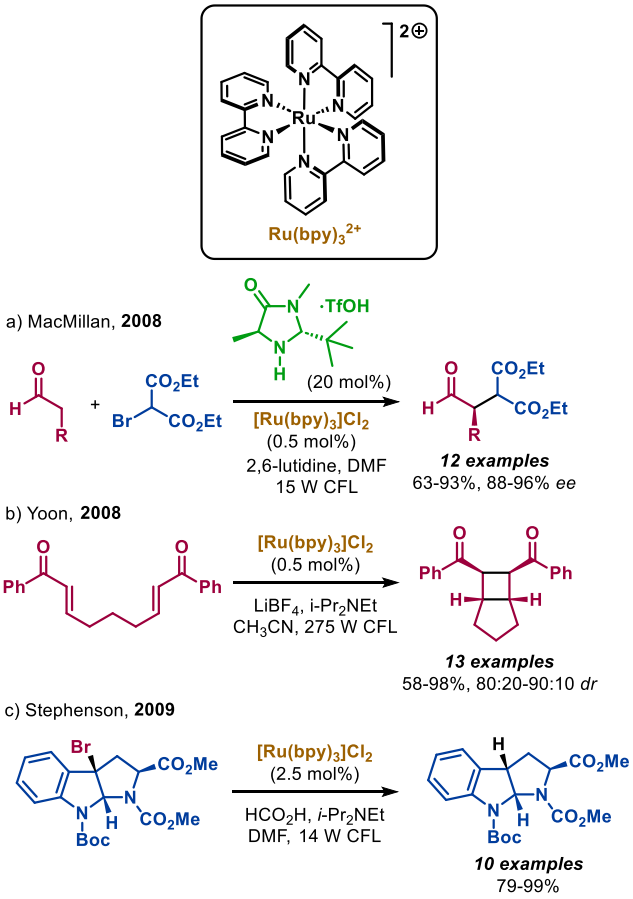

Scheme 1. Renaissance of organic photoredox catalysis.

Simpler approaches based on mass metrics are commonly favored in academia and in the pharmaceutical industry, and they are normally implemented using also empirical data on energy consumption, costs, and safety considerations.[9] In this context, it is worth mentioning that Antenucci, Renzi and co-workers recently conducted a critical examination of the mass metrics

associated with the synthesis of the most commonly used asymmetric organocatalysts.[10] They found that a significant amount of waste is generated during the preparation of these catalysts, which may have a significant impact on the efficiency and sustainability of the overall catalytic process. In this paper, we will use the same quantitative approach to assess the impact of waste generated during the preparation of the most used photoredox catalysts, as well as the overall sustainability of some selected photocatalytic processes promoted by these catalysts, providing direct comparisons to the classical synthetic routes.

1.1. Mass Metrics

The concept of green chemistry firmly developed around the twelve principles proposed by Anastas and Warner in 1998,[11] primarily emphasizing pollution prevention and safety through the reduction in both the use and the generation of hazardous substances. The twelve principles of green chemistry are mainly conceptual and propose Atom Economy (AE) as the only quantitative parameter for assessing the environmental sustainability of a chemical transformation. Originally proposed by Trost in 1991,[12] AE uses stoichiometry indexes and molecular weights to calculate the maximum theoretical efficiency achievable for a specific reaction (Figure 1), concentrating only on the efficient utilization of reagents. The problem of waste management in the chemical industry prompted Sheldon to propose the Environmental factor (E) in 1992,[13] as a metric to evaluate the mass amount of waste produced in a chemical process (Figure 1).

$$AE = \frac{p \cdot MW_{product}}{\sum_{i=0}^{n} r_i \cdot MW_{reagent}} \qquad E = \frac{\sum_{i=0}^{n} b_i \cdot MW_{by\text{-}product}}{p \cdot MW_{product}}$$

$$E = \frac{1 - AE}{AE}$$

based on MW

$$E = \frac{\text{mass of waste - isolated mass of product}}{\text{isolated mass of product}}$$

$$RME = \frac{\text{isolated mass of product}}{\text{total mass of all chemicals used}}$$

$$SF = \frac{\text{mass of reagents employed}}{\text{stoichiometric mass of reagents}}$$

$$MRP = \frac{1}{1 + \frac{y \cdot AE \cdot (\text{mass of all chemicals employed})}{SF \cdot (\text{isolated mass of product})}}$$

$$RME = \frac{y \cdot AE \cdot MRP}{SF} \qquad PMI = \frac{1}{RME} = E + 1$$

based on mass

Figure 1. Definitions and main relationships between green metrics.

After these seminal proposals, several alternative mass-based metrics have been introduced to assess the environmental impact of chemical processes.[14] Among these, Reaction Mass Efficiency (RME) and Process Mass Intensity (PMI), first proposed by Curzon at GlaxoSmithKline (GSK) in 2001[15a] and redefined by Andraos in 2005,[15b] can be considered the modern equivalents of AE. RME is calculated as the ratio between the isolated mass of the desired product and the total mass of all chemicals used, including reagents, catalysts, solvents, and auxiliary materials employed in work-up, isolation and purification steps. RME is directly related to Trost's AE through the values of chemical yield (y), Stoichiometry Factor (SF, a function of excess reagents used) and of the Material Recovery Parameter (MRP, related to the mass of all solvents, catalysts and auxiliary materials used). RME exactly equals AE in an ideal reaction where no excess reagents are used (SF = 1), with a 100% chemical yield (y = 1) and when all solvents, catalysts and auxiliary materials are either fully recovered or not used at all (MRP = 1). PMI on the other hand is defined as the ratio between the total mass of all chemicals used in a process and the isolated mass of the desired product, being essentially the exact reciprocal of RME. Just as AE and E based on molecular weights are mathematically related according to the Lavoisier's law of conservation of mass, RME and PMI are mathematically related to mass-based E, being their definitions the two sides of the same coin (Figure 1).[16]

Arianna Quintavalla got the PhD in Chemistry in 2004 at the University of Bologna (Prof. G. Cainelli) with a thesis on the synthesis of new β-lactams as enzymatic inhibitors and antibiotics. In 2009 she joined the research group of Prof. C. Trombini first as Research Technologist and then as Assistant Professor. In 2022 AQ has been appointed Associate Professor at the Dep. of Chemistry "G. Ciamician" at UNIBO. Her current research interests span from stereoselective synthesis of heterocyclic compounds, design and synthesis of new organocatalysts, development of novel and sustainable photoredox catalytic processes.

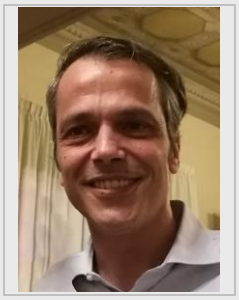

Marco Lombardo received the PhD in Chemistry in 1999 from the University of Bologna, under the supervision of Prof. Claudio Trombini, working in the field of organomercury and organoboron chemistry. He was appointed Research Associate in 1999 and Associate Professor in 2010 at the Department of Chemistry "G. Ciamician" of the University of Bologna. His current research interests are focused on the development of new stereoselective synthetic methodologies and catalytic protocols for the synthesis of molecules with practical applications.

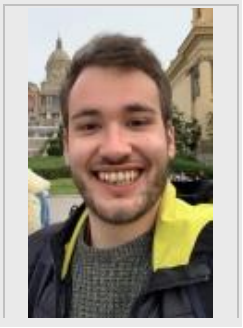

Davide Carboni received his BSc (2018) and MSc (2020) in Chemistry from the University of Bologna. After a short period at ICIQ (ES) as postgraduate trainee, he joined the PhD programme of the University of Bologna under the supervision of Profs. Marco Lombardo and Arianna Quintavalla. His research interests deal with the development of new photocatalytic methods in organic synthesis.

2. Sustainability in Photoredox Catalysis

A primary challenge in attempting to compare the sustainability of different synthetic pathways using quantitative mass-based metrics (such as PMI, RME or E) derives from the fact that experimental procedures reported in peer-reviewed journals often lack essential details, particularly regarding the mass amounts of materials used in work-up, isolation and purification stages. For example, the volume of extraction and purification solvents, including water, the mass of filtering agents (e.g., Celite), of drying agents (e.g., Na_2SO_4, $MgSO_4$) and of flash-chromatography stationary phases (e.g., SiO_2), are almost invariably not reported. On the contrary, all the necessary experimental details are typically provided for the reaction step, up to the quenching stage. Clearly, in the absence of this information, accurate values for PMI, RME, or E cannot be calculated for the entire process, and in most cases, accurate values are only available for the reaction stage.

A second challenge is related to the choice of where to begin the analysis of a synthetic plan. In many cases, starting materials and catalysts employed are described as readily or commercially available. However, it is important to remember that every chemical must be prepared, using a defined synthetic plan characterized by its own efficiency and waste generation. This is a very complex problem with no simple solution. In this context, we will analyze the reactions for the preparation of commonly used photocatalysts, as well as some selected frequently employed photoredox protocols, using the procedures as reported in the original papers. Nevertheless, the reader should be fully aware of the aforementioned limitations when comparing the efficiency and sustainability of different synthetic pathways.[16]

2.1. Photocatalysts Synthesis

Alongside the quantitative values of yield (y), Atom Economy (AE), Stoichiometric Factor (SF or 1/SF) and Process Mass Intensity (PMI), each process will be qualitatively evaluated[9b] based on the nature of the solvents employed, the reaction temperatures and times (energy requirements), the eventual use of rare and costly elements and the presence of critical hazard statements relative to reagents employed or generated waste.

Solvents. Some pharmaceutical companies have long established an internal classification of solvent greenness in the production of active pharmaceutical ingredients (APIs). Unfortunately, there are cases where conclusions do not agree in these guidelines, reflecting different subjective perspectives of the proposers.[9b] The CHEM21 consortium has more recently revisited the conclusions of some of these guides, producing a new, comprehensive solvent selection guide, that will be used in this Review. Solvents are categorized into four groups: Recommended, Problematic, Hazardous and Highly Hazardous, and color-coded accordingly as green, yellow, red and dark red.[17]

Temperatures. The accurate calculation of energy requirements for a chemical transformation can be quite challenging. In a laboratory setting, the use of relatively low-power light sources (10-40 W), such as compact fluorescent lamps (CFLs) or light-emitting diodes (LEDs), is comparable to the energy requirement of a typical magnetic stirrer (motor power 10-50 W). On the contrary, heating a reaction to high temperatures (above 140 °C) or cooling it to low temperatures (below −20 °C) is a highly energy-demanding operation. In this Review, a reaction in the 0-70 °C interval will be considered under mild conditions and color-coded as green. Reactions within the industrially acceptable temperature range (between −20 and 0 °C and between 70 and 140 °C) will be color-coded as yellow, while those outside of these ranges will be considered red.[9b]

Rare elements. The impact of using rare and costly elements in a synthetic pathway can be qualitatively evaluated by considering the risk of their depletion over a specified time interval, considering the current availability, their extraction rate and usage, with the assumption that no new unknown reserves will be discovered in the future. Accordingly, metals such as Ruthenium, Rhodium, Silver, Iridium, Platinum, Gold, Zinc and Indium will be color-coded as red (5-50 years remaining until depletion), while metal such as Cobalt, Nickel, Copper and Palladium will be color-coded as yellow (50-500 years remaining until depletion).[9b]

Hazard statements. According to the GHS (Global Harmonized System) classification, reagents and waste categorized as fatal, highly explosive, potential carcinogenic or mutagenic and very toxic to aquatic life (Signal Word: Danger) will be considered very hazardous and color-coded as red.

Mass-based metrics. *Organic Synthesis* is one of the few journals that require experimental procedures to be reported with full details, making the reported procedures particularly suitable for quantitative mass-based metrics analysis. The detailed procedures for the preparation of five photoredox catalysts (**A**-**E**, Figure 2) were found in this journal, specifically for $Ir(ppy)_3$ (**A**, ppy = 2-phenyl-pyridine),[18] $[Ir\{dF(CF_3)ppy\}_2(bpy)]PF_6$ (**B**, $dF(CF_3)ppy$ = 3,5-difluoro-2-[5-(trifluoromethyl)-2-pyridinyl),[19] $[Ir\{dF(CF_3)ppy\}_2(dtbbpy)]PF_6$ (**C**, dtbbpy = 4,4'-bis(*tert*-butyl)-2,2'-bipyridine),[19] $[Ru(bpz)_3][BArF]_2$ (**D**, bzp = 2,2'-bipyrazyl, BArF = bis(tetrakis(3,5-bis(trifluoromethyl)phenyl)borate)),[20] and 4CzIPN (**E**, Cz = 2,4,5,6-tetra(9H-carbazol-9-yl), IPN = isophthalonitrile).[21]

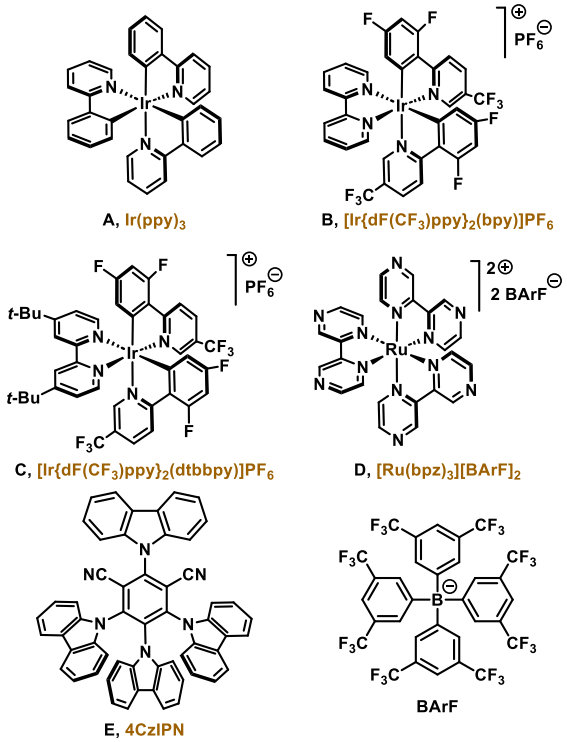

Figure 2. Structures of photocatalysts **A**-**E**.

The metrics calculated for the synthesis of photocatalysts **A**-**E** are reported in Table 1. Cumulative values are reported in the case of multi-step preparations.[22]

Table 1. Mass-based metrics for the synthesis of photocatalysts **A**-**E**.[a]

Catalyst	Steps	y	AE	SF	PMI
A	1	0.91	0.86	2.83	3658
B	3	0.46	0.70	3.70	1140
C	3	0.52	0.72	2.04	1063
D	2	0.34	0.60	2.23	2738
E	1	0.88	0.49	1.07	207

[a] Cumulative values for multi-step syntheses.

Synthesis of Ir(ppy)$_3$ **(A).** Ir(ppy)$_3$ is prepared in a single step by reacting $IrCl_3$ with a large excess of 2-phenylpyridine (SF = 2.83), in water at 205 °C for 48 h, yielding 91% of the isolated product. However, despite the rather favorable value of AE (0.86), the process is characterized by a rather large PMI (~3.66 Kg of chemicals/g product), primarily due to the large amount of water and organic solvents employed in the isolation and purification stage. The use of water as a benign reaction solvent is somewhat counterbalanced by the large volumes of dichlorometane (DCM, ~660 g/g product) and hexane (~310 g/g product) used, both of which are marked as hazardous (red flag) solvents. Additionally, the process raises a red flag in terms of its energetic requirements, as the reaction is done well above the solvent refluxing temperature for an extended time (205 °C, 48 h). Furthermore, it's worth noting that iridium is considered a rare and expensive element, which also contributes to the overall cost and sustainability concerns of this synthetic procedure (red flag).

Synthesis of [Ir{dF(CF$_3$)ppy}$_2$(bpy)]PF$_6$ **(B) *and [Ir{dF(CF$_3$)ppy}$_2$ (dtbbpy)]PF$_6$*** **(C).** Photocatalysts **B** and **C** are prepared in a three-steps synthetic sequence, with the first two steps being identical and differing only in the choice of the 2,2'-bipyridine ligands used in the third step. These two processes are thus very similar and have similar metrics, notably a relatively high value of PMI (~1.14 and ~1.06 Kg of chemicals/g product, respectively). In both cases, the first step is the Pd(PPh$_3$)$_4$ catalyzed Suzuki cross-coupling between (2,4-difluorophenyl)boronic acid and 2-chloro-5-(trifluoromethyl)pyridine, for the preparation of the 2-(2,4-difluorophenyl)-5-(trifluoromethyl)pyridine ligand (dF(CF$_3$)ppy) in 91% yield. The reaction is carried out in a 5:1 mixture of benzene and ethanol (~5 g/g product), with a significant amount of DCM being used during the purification stage (~170 g/g product). It's important to note that benzene is now considered a banned solvent (dark red flag), and DCM is classified as hazardous solvent (red flag). Additionally, the reaction conditions, involving a temperature of 70-75 °C and a long reaction time (72 h), make this step only partially sustainable (yellow flag). In the second step, $IrCl_3$ (red flag) is reacted with a slight excess of dF(CF$_3$)ppy, in a 2:1 mixture of 2-ethoxyethanol/water (~32 g/g product) at 120-125 °C for 48 h (yellow flag), affording the desired complex in 76% yield. Methanol (~42 g/g product) and pentane (~10 g/g product) are the primary solvents used for work-up and purification, both of which are listed as hazardous solvents (red flag). In the final step, the iridium dimer is reacted with the desired 2,2'-bipyridine at 150 °C for 48 h (red flag) in a 2:3 mixture of ethylene glycol (yellow flag) and water (~90-95 g/g product). Finally, the chlorine anion is exchanged using a large excess of NH_4PF_6 (~25 equivalents) in water, giving **B** in 66% and **C** in 74% yield. Once again, substantial quantities of organic solvents are used in the isolation and purification steps, mainly pentane (~78 g/g product) and hexane (~41 g/g product) in the first case, and hexane (~128 g/g product) in the second case (red flag). Overall, the relatively harsh reaction conditions in all three synthetic steps, the use of significant excesses of some reagents, and the substantial quantities of hazardous organic solvents employed, together contribute to the unsustainability of this process.

Synthesis of [Ru(bpz)$_3$][BArF]$_2$ **(D).** [Ru(bpz)$_3$][BArF]$_2$ is prepared in two steps. In the first step, a palladium-catalyzed Suzuki homo-coupling of 2-iodopyrazine is used to prepare the desired ligand, 2,2'-bipyrazine. This process is characterized by a low value of AE (0.26), primarily due to the high molecular weight of iodine acting as a leaving group, compared to the molecular weight of the desired product. The reaction is carried out in *N*,*N*'-dimethylformamide (DMF, ~52 g/g product), at 100 °C for 2 h (yellow flag), to give the desired product in 74% yield. Large amounts water (~240 g/g product) and ethyl acetate (AcOEt, ~245 g/g product) are used in the purification stage, but both solvents are listed as recommended in solvent selection guides. However, it's worth noting that DMF, used in the reaction stage, is classified as a hazardous solvent (overall yellow flag). In the second step, $RuCl_3$ (red flag) is reacted with 2,2'-bipyrazine in a mixture of ethylene glycol, water and methanol (67:25:8, ~150 g/g product) at 214 °C for 3 h (red flag). Finally, the anion is exchanged with NaBArF in methanol, to afford the desired photocatalyst in 46% yield. In this second step, a notably high PMI value is obtained, primarily due to the significant quantities of hazardous organic solvents required for product purification. This aspect makes the overall procedure not sustainable, particularly due to the use of DCM (~880 g/g product) and benzene (~70 g/g product).

Synthesis of 4CzIPN **(E).** 4CzIPN is prepared in 88% yield by reacting tetrafluoroisophthalonitrile with a slight excess sodium hexamethyldisilazide (NaHMDS) and of carbazole in THF (~10 g/g product, yellow flag) at 65 °C for 24 h. During the work-up and purification stages, substantial quantities of hazardous organic solvents, particularly diethyl ether (Et_2O, ~40 g/g product) and chloroform (~146 g/g product), are employed (both color-coded as dark red). Despite the unfavorable value of AE (0.49), the use of a small excess of reagents (SF = 1.07) and the relatively small volumes of organic solvents used for the isolation and purification of catalyst **E** contribute to give the lowest value of PMI (207 g chemicals/g product) in the entire series.

The overall results obtained for the preparation of photocatalysts **A**-**E** are graphically summarized in Figure 3.

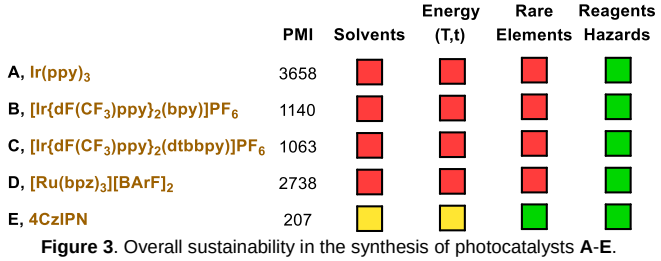

Figure 3. Overall sustainability in the synthesis of photocatalysts **A**-**E**.

The 9th principle of green chemistry highlights catalysis as a fundamental strategy to enhance energy efficiency, promote atom economy, reduce toxicity, and minimize waste, thereby reinforcing and supporting all the other green chemistry principles.[11] Consequently, being catalytic is often used as a

primary criterion for recognizing a process as environmentally sustainable. However, this perspective sometimes neglects the waste associated with the use of chemicals in catalytic amounts. Given the PMI values just calculated for the synthesis of photocatalysts **A**-**E**, one should reconsider this assessment carefully, without automatically assuming the inherent green advantages of catalysis. Moreover, one of the most employed criteria for asserting the greenness of a catalytic protocol is related to the potential catalyst recyclability, often disregarding the quantification of waste generated during the recycling stage, and completely neglecting the sustainability of the synthetic protocols employed in the preparation of the catalyst.[10] Even if an excellent product selectivity is obtained at room temperature, without using large excesses of reagents, the overall catalytic process may not be easily scaled to an industrial level if the catalyst itself cannot be conveniently prepared.

The mass-based metrics associated to the use of a catalyst employed in a specific amount (mol%) can be readily calculated by considering the PMI value associated with the catalyst preparation (PMI_{Cat}), the molecular weight of the catalyst (MW_{Cat}), the molecular weight of the product (MW_P), and the yield of the reaction (y). To provide a quantitative understanding of how the PMI value associated to the synthesis of a catalyst can influence the overall efficiency of a catalytic protocol, we have calculated some theoretical values for different scenarios, reported in Table 2.

Table 2. PMI contribution from the catalyst synthesis to the overall mass efficiency of a catalytic protocol with MW_P = 250 and y = 0.8.

$$PMI = PMI_{Cat} \cdot \frac{MW_{Cat}}{MW_P} \cdot \frac{1}{y} \cdot \frac{mol\%}{100}$$

Catalyst	**PMI_{Cat}**	**mol%**	**0.1**	**0.5**	**1**	**5**	**10**	**20**
A	3658	**PMI**	12	60	120	599	1198	2396
B	1140	**PMI**	6	29	58	288	576	1151
E	207	**PMI**	0.8	4	8	41	82	163

From the inspection of the values presented in Table 2, it becomes apparent that the waste generated during the synthesis of a catalyst can significantly influence the overall mass-efficiency of a catalytic protocol, particularly when the value of PMI_{Cat} is large, even if the catalyst is used in small amounts. For example, $Ir(ppy)_3$ (**A**) is tipically used in just 1 mol% amount, but it can still contribute hundreds of grams to the total waste produced. Conversely, the organic photocatalyst 4CzIPN (**E**), characterized by a much lower PMI_{Cat} value, may have a relatively minor impact when used in 1 or 2 mol% amounts. However, its contribution to waste production can dramatically increase when used in larger amounts, as is often the case with organic dyes. To accurately assess a catalyst contribution to the overall waste generated in a catalytic process, we will employ the global PMI factor (PMI_G) in this Review. This approach will provide a more comprehensive perspective on the overall sustainability of a chemical catalytic transformation.

The data acquired for the synthesis of photocatalysts **A**-**E** can also be used for critically assessing the distinct contributions of solvents to the overall PMI values. Specifically, the quantity (E = PMI − 1) and the nature of waste generated by solvents during the reaction (R), the work-up (WU) and the purification (P) stages. The results of this analysis are detailed in Table 3.

Table 3. Contribution of solvents to the total waste (E_{TOT}) in the synthesis of photocatalysts **A**-**E**.[a]

Catalyst (E_{TOT})	E_R	E_{WU} H_2O	E_{WU} Organic	E_P Organic
A (3657)	504 (14%)	2129 (58%)	665 (18%)	307 (8%)
B (1139)	153 (13%)	247 (22%)	255 (22%)	411 (36%)
C (1062)	137 (13%)	268 (25%)	184 (17%)	419 (39%)
D (2737)	246 (9%)	238 (9%)	454 (17%)	1318 (48%)
E (206)	12 (6%)	0	186 (90%)	7 (3%)

[a] R = Reaction stage; WU = Work-up stage; P = Purification stage.

Upon examining the values presented in Table 3, it becomes clear that the primary source of waste in synthetic protocols derives from the solvents employed, ranging from 83% for **D** to 99% for **E**, and particularly during the work-up and purification stages. The remainder of the mass is accounted for by the contribution from reagents and auxiliary materials, making up the total waste generated. In contrast, there is a relatively smaller contribution from all chemicals employed in the reaction stage, where, once again, the mass of reaction solvents plays the most significant role. Since the protocols analyzed for the synthesis of other photocatalysts and for the selected catalytic reactions are sourced from papers where work-up and purification details are not always thoroughly reported, it is worthwhile to assess the percentage of chemicals used in these stages in comparison to the reaction phase. These results are outlined in Table 4, clearly indicating that 86% to 94% of all waste produced derive from the work-up and purification stages, with an average value of 88%.

Table 4. Percentage contribution of all chemicals to the total waste (E_{TOT}) in the synthesis of photocatalysts **A**-**E,** during the reaction, the work-up and the purification stages.[a]

Catalyst (E_{TOT})	E_R	E_{WU}	E_P	E_{WU+P}
A (3657)	13.9%	77.7%	8.4%	86.1%
B (1139)	14.4%	47.0%	38.6%	85.6%
C (1062)	13.4%	45.0%	41.6%	86.6%
D (2737)	9.4%	25.7%	64.9%	90.6%
E (206)	6.5%	90.3%	3.2%	93.5%

[a] R = Reaction stage; WU = Work-up stage; P = Purification stage.

We further analyzed the preparation procedures for $[Ru(bpy)_3]Cl_2 \cdot 6H_2O$ (**F**),[23] $[Ru(bpy)_3][PF_6]_2$ (**G**),[24] $[Ir(bpy)_2(dtbbpy)]PF_6$ (**H**),[25] DCQ (**I**, DCQ = 2,3-di(9*H*-carbazole-9-yl)quinoline),[26] $MesAcrPhBF_4$ (**J**, Mes = mesityl, Acr = acridinium),[27] $MesAcrClO_4$ (**K**),[28] Eosin Y (**L**),[29] and Cl-TXO (**M**, TXO = thioxanthone),[30] and the results obtained are reported in Figure 4.

In the preparation of ruthenium photocatalysts (**F**, **G**) and Eosin Y (**L**), the only missing information was relative to the mass amounts of auxiliary materials used during the work-up and purification stages. However, all the solvents employed were explicitly specified. Therefore, the PMI values obtained for these three procedures should deviate only slightly from the true values. Conversely, the metric values for organic photocatalysts **I-K**, and **M** were calculated only for the reaction stage, while for iridium photocatalyst **H** only the data for the first reaction step were reported in detail. Referring to the values calculated in Table 4, it is not implausible that the actual PMI values for these photocatalysts could be 5 to 10 times larger, when compared to the calculated ones. Finally, it should be mentioned once again that the syntheses of rare metals photocatalysts **F**-**H** require very-high temperatures for extended reaction times, while the preparation of organic catalyst **J** uses the very hazardous iodomethane (H301+H331) in large excess, and very toxic 2,3-dichloroquinoxaline (H301) is used as a starting material in the preparation of the organic dye **I**.

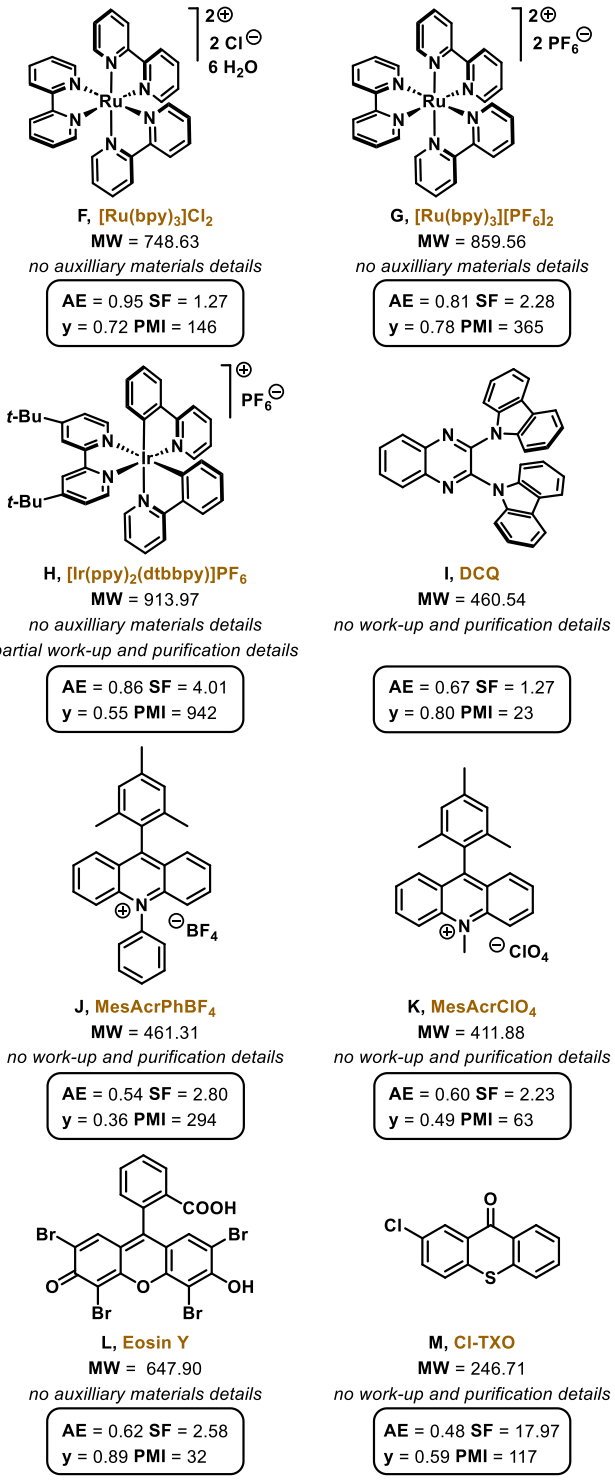

Figure 4. Cumulative metrics for the synthesis of photocatalysts **F**-**M**.

2.2. Photoredox Catalytic Reactions

To assess the sustainability of photoredox catalytic methodologies applied to the construction of organic molecules, we selected some reaction classes that have been extensively studied in this field. Within these classes, we evaluated specific model transformations under varying reaction conditions, quantitatively comparing factors such as Atom Economy (AE), Stoichiometric Factor (SF), and Process Mass Intensity (PMI). Additionally, we considered the nature of the catalyst, solvent toxicity, reaction time, and temperature to comprehensively

assess the overall sustainability profile of each process. Finally, a comparison with an analogous transformation not promoted by light was also made, aiming to evaluate the real advantages of the photocatalytic approaches in terms of process sustainability.

Unlike the photocatalysts syntheses previously discussed, the analysis of the photocatalyzed reactions will be conducted without considering the work-up and purification steps, for which sufficient details are not described in the procedures reported in the literature.

2.2.1 α-Amine Functionalization

Among the various strategies to generate reactive radical species, the single electron oxidation of neutral organic compounds is one of the most studied. In particular, being amines very electron-rich, they were largely exploited as precursors of radical cations. The C−H bonds adjacent to the positive nitrogen atom are remarkably acidic (pK_a ~ 8) and their easy deprotonation provides the corresponding α-aminoalkyl radical. On the other hand, α-aminoalkyl radicals are more readily oxidized than the corresponding amines ($E_{1/2}$ = −1.03 V vs SCE and $E_{1/2}$ = +1.15 V vs SCE, respectively). Therefore, the iminium ions can be rapidly obtained with an excess of oxidant. Because of these peculiar redox properties, amines can be functionalized at α-position with both electrophiles (exploiting the nucleophilic α-aminoalkyl radical) and nucleophiles (exploiting the electrophilic iminium ion). Visible light-mediated photoredox catalysis gives the opportunity to achieve the intermediate amino radicals under mild conditions and the α-amino functionalization has become one of the most studied transformations.[31]

2.2.1.1 α-Amine Arylation

We selected the α-amino arylation as example of functionalization occurring through α-amino radical formation when promoted by light, leading to a structural motif present in medicinally relevant compounds[32] including top-selling pharmaceuticals.[33] In 2011, MacMillan and co-workers published a seminal work describing the discovery of the first photoredox amine C–H arylation, requiring easily available starting materials, mild conditions and operationally simple protocols (Scheme 2).[34]

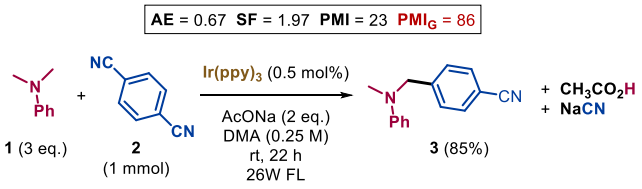

Scheme 2. Photocatalytic α-amino arylation protocol proposed by MacMillan in 2011.

We analyzed the green chemistry metrics of the reaction carried out on *N*,*N*-dimethylaniline **1** and 1,4-dicyanobenzene **2** using tris[2-phenylpyridinato-C^2,N]iridium(III) (**A**) as photocatalyst. The AE of the process (0.67) is limited by the unavoidable generation of by-products (AcOH and NaCN) and the SF (1.97, 1/SF = 0.507) is strongly penalized by the use of excess of amine **1** (3 eq.) and base (2 eq.) (Figure 5).

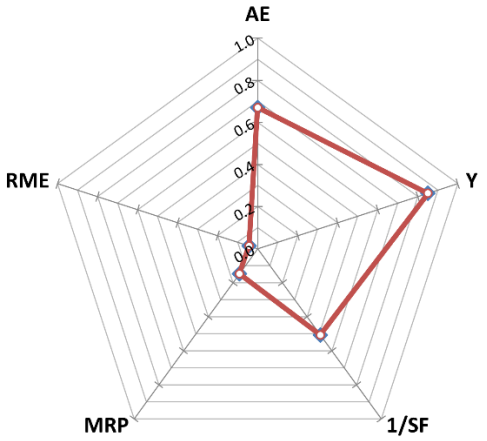

Figure 5. Performance pentagon for the α-amino arylation proposed by MacMillan in 2011.

Despite the low catalyst loading (0.5 mol%) and the high yield (85%), the resulting PMI shows that 23.4 g of materials are required, de facto generating 22.4 g of waste, to produce 1 g of product **3**. Furthermore, even though catalyst **A** is used in very small amounts, the quantity of waste generated during its preparation significantly exceeds the waste produced during the reaction stage, nearly quadrupling the value of the global PMI (PMI$_G$ = 86).

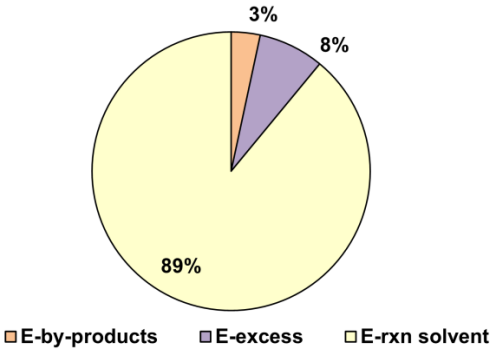

Figure 6. Distribution of the total waste of the MacMillan's synthesis of **3**.

The reaction waste (Figure 6) consists of reagents excesses (8%), by-products (3%) and solvent (89%), which, as expected, plays the major role. In fact, the process efficiency could improve approximately 7 times if the solvent was recycled (PMI = 3.5 vs 23.4). Concerning the reaction medium, the authors proposed *N*,*N*-dimethylacetamide (DMA) as the best one. However, it is toxic[35] and it is classified as undesirable reaction solvent according to the widely accepted solvents sustainability guides[17a,36] and the green chemistry principles (red flag). As already demonstrated, solvents represent the main source of waste generated by a chemical transformation, therefore their dangerousness heavily affects the overall sustainability profile of the process. Regarding the safety of this peculiar reaction, it is relevant to mention that a stoichiometric amount of very toxic NaCN[37] is produced (H314, H300+H310+H330, H372). The nature of the photocatalyst can also significantly contribute to

determine the economic and environmental impact of a chemical transformation, and, eventually, its large scale applicability, especially when metal-complexes based on expensive and scarcely available elements are employed.[38] In the MacMillan's α-amino arylation, the reaction is promoted by $Ir(ppy)_3$ (**A**) and iridium is among the rarest elements on Earth (red flag). Moreover, the environmental impact of organometallic photocatalysts can be remarkable, being slowly degraded and acting as fluorescent pollutants. As a consequence, one of the prevailing challenges is the recycling of rare metal-based photocatalysts, leading to environmental and economic benefits.[39]

Recently, we contributed to this field by proposing an improved protocol for the photocatalytic α-amino arylation,[40] in which *i)* the toxic polar aprotic medium was replaced with the greener solvents 1-butyl-2-pyrrolidone (NBP)[41] or 2-pyrrolidone (NHP),[42] *ii)* the solvent NHP and the commercially available costly photocatalyst $Ir(ppy)_3$ were both recycled, *iii)* the photocatalyst loading was lowered to 0.05 mol% maintaining excellent performance (Scheme 3).

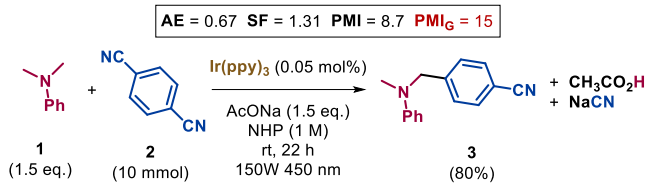

Scheme 3. Photocatalytic α-amino arylation protocol proposed by us in 2023.

With the same AE (0.67) the process efficiency results improved in several aspects. First, the SF (1.31 vs 1.97) due to the lowered excess of employed reagents (amine and base). Moreover, the reaction concentration quadrupled (1 M vs 0.25 M). These variations lead to a substantial reduction of the PMI (8.7 vs 23.4) with a marked decrease in the mass of produced waste (7.7 vs 22.4 g for each g of desired product; 6.3 vs 19.9 g of solvent). In this protocol the solvent NHP was effectively recycled allowing to achieve the excellent PMI value of 2.4 (MRP = 0.28 without recycling, MRP = 0.999 with recycling, Figure 7).

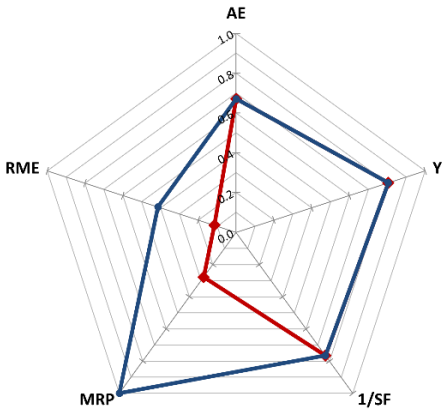

Figure 7. Comparison between performance pentagons with (blue line) and without (red line) solvent recycling for the α-amino arylation proposed by us in 2023.

Regarding the Ir-based photocatalyst **A** (red flag), reducing its amount to 0.05 mol% from the original 0.5 mol% had a significant impact on the amount of waste generated, resulting in a much lower global PMI value (PMI_G: 15 vs 86). This improvement enhances the overall process sustainability in terms of costs and environmental impact. Finally, it's important to highlight the clear advantage of replacing a highly toxic solvent (DMA) with a more environmentally friendly one (NHP or NBP) (yellow flag and green flag, respectively).

Having analyzed two different photocatalytic protocols for the α-arylation of amines, we turned our attention to a methodology not promoted by light, but capable of providing the same product **3**. We found a procedure very recently proposed by Fan *et al.* that yields the same product by forming a different bond (C-N) through a different mechanism (Scheme 4).[43]

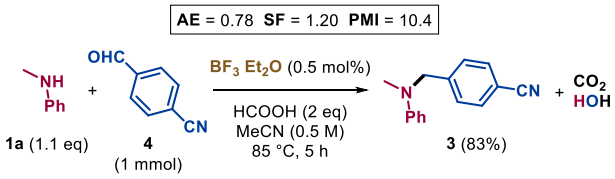

Scheme 4. Thermal synthesis of product **3** proposed by Fan in 2021.

The AE is higher compared to the photoredox strategy (0.78 vs 0.67), primarily due to the generation of low molecular weight by-products. Additionally, the excess of low molecular weight formic acid contributes to the smaller SF value (1.20), which is significantly better than that of the MacMillan's procedure (1.97) and similar to our value (1.31). The PMI (10.4) is slightly worse than our photocatalytic procedure, resulting in water and the greenhouse gas CO_2 as the only by-products (Figure 8 vs Figures 5 and 7).

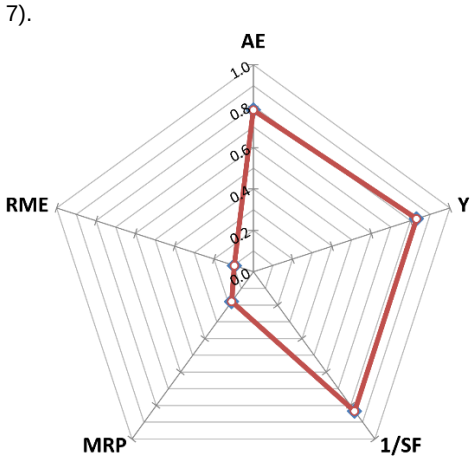

Figure 8. Performance pentagon for the thermal synthesis proposed by Fan in 2021.

The solvent accounts for 91% of the total waste mass, as the reaction mixture is relatively concentrated (0.5 M). Recycling the solvent could potentially reduce the PMI to 1.9, the lowest value compared to both the described photoredox methodologies. In terms of process safety, it must be noted that the reaction solvent (MeCN)[44] presents some concerns (yellow flag). The favorable metrics in terms of sustainability are partly

counterbalanced by the high reaction temperature (85 °C, yellow flag) that must be maintained for a relatively extended period (5 h).

The green chemistry metrics calculated for the syntheses of α-aryl amine **3** are compared in Table 5.

Table 5. Comparison between the green chemistry metrics of the protocols for the synthesis of α-aryl amine **3**.[a]

	Scheme 2[34]	Scheme 3[40]	Scheme 4[43]
AE	0.67	0.67	0.78
SF	1.97	1.31	1.21
Yield [%]	85	80	83
PMI	23	8.7	10.4
PMI_{SR}	3.5	2.4	1.9
PMI_G	86	15	-
Time	22 h	22 h	5 h
Temp [°C]	rt	rt	85

[a] PMI_{SR} = PMI with solvent recycled; PMI_G = PMI including the impact of the catalyst synthesis; Temp = reaction temperature; rt = room temperature; h = hours.

This analysis shows that, for the synthesis of product **3**, the sustainability of a photoredox catalytic approach may be comparable to that of a catalytic thermal strategy, but only when low amounts of photocatalyst are used, reagents excess is reduced, a greener solvent is used and potentially recycled (Scheme 3).

2.2.1.2 α-Amine Phosphorylation

As an exemplary process for photocatalytic α-amino functionalization *via* iminium ion formation, we selected the preparation of α-aminophosphonates. These compounds, along with structurally related α-aminophosphonic acids, are considered interesting due to their biological and agromedical properties.[45] In 2018, Lei and co-workers proposed an external oxidant-free synthesis of α-aminophosphonates by combining photocatalysis and cobalt catalysis for the proton-reduction (Scheme 5).[46]

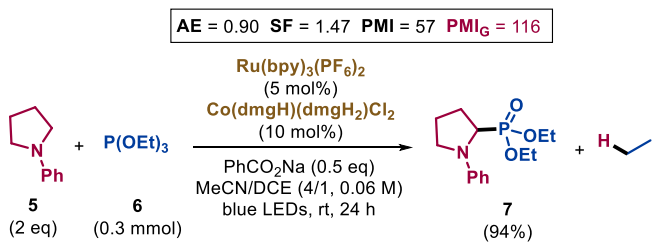

Scheme 5. Photocatalytic α-amino phosphorylation protocol proposed by Lei in 2018.

This approach has broader applicability, as the previously described photo/oxidant catalytic systems are often incompatible with *N*,*N*-dialkylanilines and other oxidant-sensitive substrates. The process is characterized by an excellent AE (0.90), deriving from the stoichiometric co-generation of low molecular weight ethane. The SF (1.47) is moderate, due to the excess (2 equivalents) of pyrrolidine **5**. Despite the excellent AE and the high yield (94%), the PMI is large (57), mainly due to the solvents' contribution (98% of the total waste mass). In fact, recycling the reaction medium would lead to a drastic reduction of the PMI (2.3), with a significant improvement of process sustainability (Figure 9). Furthermore, when accounting for the waste generated in the preparation of the required amount of catalyst **G**, the global PMI value nearly doubled (PMI_G = 116).

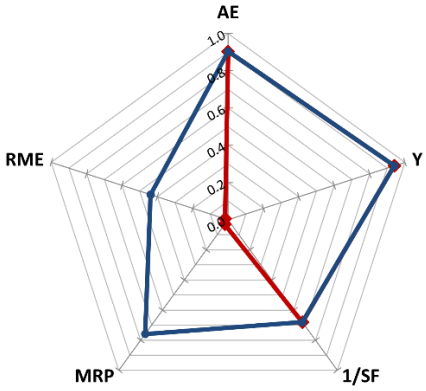

Figure 9. Comparison between performance pentagons with (blue line) and without (red line) solvent recycling for the α-amino phosphorylation proposed by Lei in 2018.

It is noteworthy that the reported reaction conditions are highly diluted (0.06M), therefore a simple increase in concentration could potentially improve the process efficiency. The last remark on the solvent concerns the high toxicity of DCE[47] (dark red flag). Regarding the tricomponent catalytic system, it must be noted that it represents 1% of the waste mass, an unusually high value. Therefore, to synthesize 1 g of product **7**, 0.55 g of catalysts are required, including 0.28 g of metal-based species (yellow flag for cobalt, red flag for ruthenium).

We compared the metal-based photoredox dual catalytic route to α-aminophosphonate **7** reported by Lei with the organic photoredox catalytic phosphorylation developed by Xu in 2021.[48] Also in this case two catalysts synergistically work, namely TsOH as a Brønsted acid and the newly synthesized donor-acceptor fluorescent molecule DCQ (2,3-di(9*h*-carbazole-9-yl)quinolone, **I**) as a photocatalyst (Scheme 6).

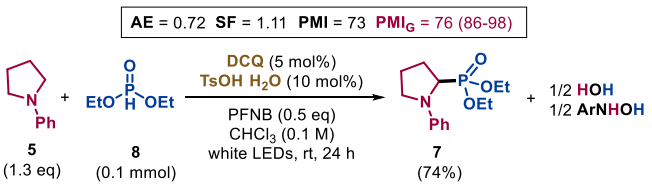

Scheme 6. Photocatalytic α-amino phosphorylation protocol proposed by Xu in 2021.

This metal-free approach is characterized by an excellent SF (1.11) due to the low excess (0.3 equivalents) of employed amine **5**. However, the AE of the process (0.72) suffers from the need to use the high molecular weight co-reactant PFNB (pentafluoronitrobenzene) to scavenge the hydrogen atoms stoichiometrically generated in the transformation. In fact, to obtain 1 g of product **7**, 0.51 g of PFNB are required, which generate approximately the same amount of waste. The value of PMI (73) is very unfavorable and, as expected, it is mainly due to the solvent contribution (98% of the waste mass). This result arises not only from the diluted reaction conditions (0.1 M) but also from the high molecular weight of the chlorinated solvent. Solvent recycling could lower the PMI down to 2.3, the same value achievable with the metal-based protocol proposed by Lei (Scheme 5). This finding shows that, excluding the solvent, the two strategies are equivalent. On the other hand, the impact of waste deriving from the preparation of the photocatalysts is much smaller in the second case (**I**, 20-35%), highlighting the importance of designing sustainable synthetic procedures for catalyst preparations. Regarding the use of chloroform[49] as the reaction medium, it must be underlined that it is highly toxic (dark red flag) and it would not be applicable in industrial productions.[36] Comparing the two photocatalytic methods, it can be observed that the lower environmental impact of the organic catalysts (Scheme 6) is partially counterbalanced by the higher cost of diethyl *H*-phosphonate **8** with respect to triethyl phosphite **6**.

As last protocol of α-amino phosphorylation we analyzed the thermal strategy reported by Ofial in 2010 (Scheme 7).[50]

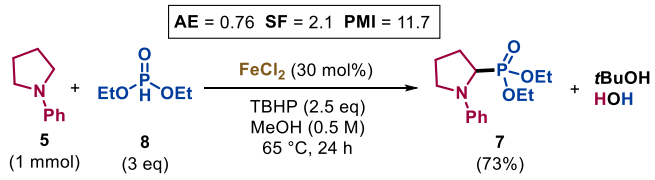

Scheme 7. Thermal α-amino phosphorylation protocol proposed by Ofial in 2010.

The co-production of *tert*-butanol and water leads to a moderate AE (0.76). However, the major weakness of this transformation lies in the employed large excess of two reactants (**8** and TBHP), as highlighted by SF (2.1). The catalyst is also used in high loading (30 mol%). Despite these flaws, the PMI is acceptable (12), remarkably lower than those of the photocatalytic α-phosphorylation protocols (Schemes 5 and 6). This good achievement is mainly due to the low amount of solvent used in this approach (0.5 M), which constitutes only 72% of the reaction waste (Figure 10). In this case, a significant portion of the discarded mass derives from reagents excess (19%), by-products (7%) and catalyst (2%).

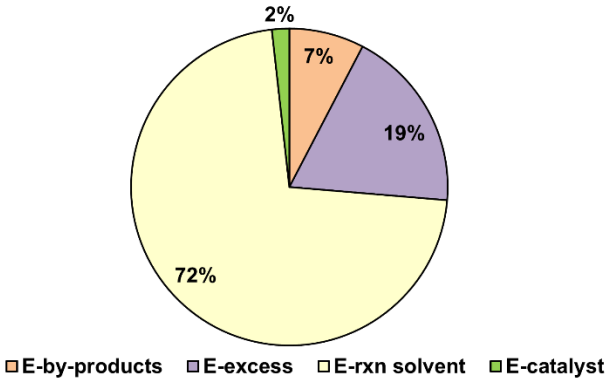

Figure 10. Distribution of the total waste of the Ofial's synthesis of **7**.

Solvent recycling would allow to achieve a PMI value of 4, superior to that of the photocatalytic protocols (2.3). This finding shows that, omitting the solvent impact, the sustainability of the visible light promoted synthetic strategies is greater. On the other hand, it is also evident that, from the perspective of the industrial application, the major weakness of the photoredox catalytic methods lies in the use of solvents. The thermal phosphorylation described by Ofial is characterized by MeOH[51] as reaction medium and TBHP[52] as oxidant (used in excess), both classified as toxic (red flags). However, the CHEM21 consortium[17a] recently classified MeOH as recommended (green flag). The metal-based catalyst ($FeCl_2$) is environmentally benign (green flag). The last remark concerns the reaction temperature: mild conditions (room temperature, green flag) characterize the photocatalytic methods, whereas the thermal approach requires heating for a long time (24 hours). However, 65 °C is within the industrially acceptable temperature range and it is color-coded as green.

Table 6 summarizes the green chemistry metrics calculated for the phosphorylation procedures leading to product **7**.

Table 6. Comparison between the green chemistry metrics of the protocols for the synthesis of α-phosphoryl amine **7**.[a]

	Scheme 5[46]	Scheme 6[48]	Scheme 7[50]
AE	0.90	0.72	0.76
SF	1.47	1.11	2.10
Yield [%]	94	74	73
PMI	57	73	12
PMI_{SR}	2.3	2.3	4.0
PMI_G	116	76 (86-98)	-
Time	24 h	24 h	24 h
Temp [°C]	rt	rt	65

[a] PMI_{SR} = PMI with solvent recycled; PMI_G = PMI including the impact of the catalyst synthesis; Temp = reaction temperature; rt = room temperature; h = hours.

2.2.2 C(sp3)-C(sp3) Bonds Formation

The formation of $C(sp^3)$-$C(sp^3)$ bonds, on a par with $C(sp^2)$-$C(sp^2)$ bonds, represents one of the main objectives of synthetic chemistry. Therefore, several different strategies have been developed over the years in search of innovative and more efficient approaches.[53] Among the recently proposed photocatalytic methods, one of the most employed involves the generation of sp^3-carbon-centered radicals as key intermediates, obtained through the displacement of C-halogen bonds.[54] As an example of application of this strategy, we reported in 2021 the visible light promoted synthesis of 2,3-dihydrofurans (Scheme 8),[55] five-membered heterocyclic scaffolds widely present in medicinally relevant compounds,[56] materials, dyes[57] and synthetic intermediates.[58] The process is redox-neutral, acting the Ir-catalyst (**A**) as both reductant and oxidant in two different steps of the catalytic cycle. The sustainability resulted improved thanks to avoiding the use of both sacrificial reactants and stoichiometric strong oxidants. Moreover, two new bonds (C-O and C-C) are formed one-pot according to a domino transformation (Scheme 8).

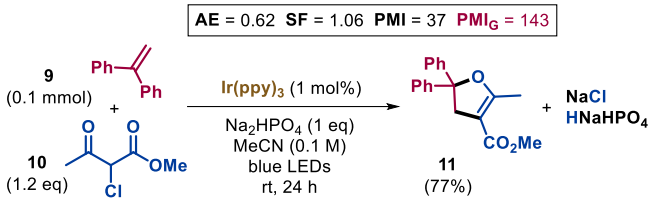

Scheme 8. Photocatalytic synthesis of 2,3-dihydrofuran **11** proposed by us in 2021.

We calculated a modest AE (0.62) due to the co-generation of NaCl and NaH_2PO_4, which, nevertheless, are environmentally benign inorganic salts. The SF value (1.06) is excellent thanks to the use of a very low excess (0.2 equivalents) of β-ketoester **10**. The PMI results acceptable (37), further improvable to 2.25 if the solvent was recycled (Figure 11). Once again, it is demonstrated that the major contribution (in this case, 97%) to the reaction waste is given by the reaction medium.

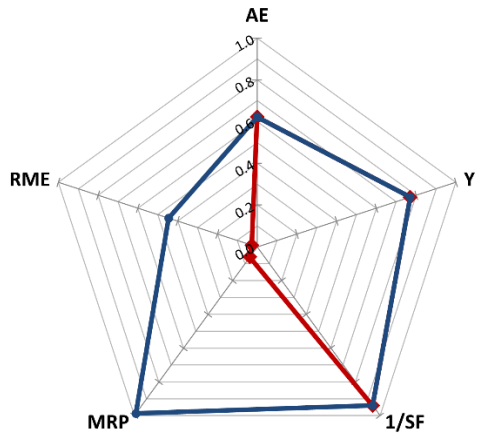

Figure 11. Comparison between performance pentagons with (blue line) and without (red line) solvent recycling for the 2,3-dihydrofuran **11** synthesis proposed by us in 2021.

The solvent of choice is MeCN, advantageous in terms of low molecular weight, recommended according to health and environment scores, but problematic in terms of safety (flammable, yellow flag).[17a,44] It can be used in the lab or in the Kilolab, but its implementation at the production scale require specific measures. As a final note, the photocatalyst is the metal based $Ir(ppy)_3$ **A** (red flag) and once again, even if used in low loading (1 mol%), the impact of the waste produced during its synthesis is considerable, almost quadrupling the value of the global PMI (PMI_G = 143).

Aiming to estimate whether the photocatalytic approach can lead to a real benefit in the sustainable synthesis of dihydrofuran **11**, we analyzed the green chemistry metrics of some thermal strategies providing the same product.

In 2015, Lei and co-workers proposed the oxidative coupling/annulation of β-ketoesters with alkenes catalyzed by iodine (Scheme 9).[59] The AE (0.51) is slightly worse than the photocatalytic approach, since three by-products are generated. Moreover, the SF (1.5) is significantly unfavorable because of the excess of both alkene **9** and oxidant TBPB.

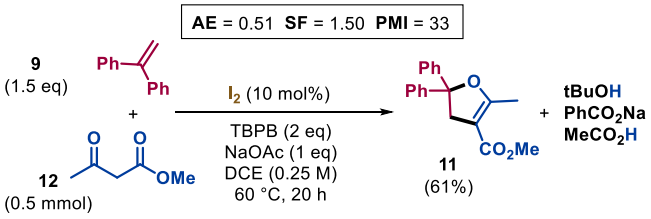

Scheme 9. Iodine-catalyzed synthesis of 2,3-dihydrofuran **11** proposed by Lei in 2015.

Despite these values of AE and SF and the moderate yield (61%), the overall PMI is acceptable (33), similar to that of the photocatalytic method (37). In this case, the efficiency improvement due to solvent recycling would correspond to PMI = 4.9, with DCE for 88% of the process waste mass. This finding proves that, omitting the solvent impact, the photocatalytic strategy is more efficient than the thermal iodine-catalyzed approach (2.25 vs 4.9). Nevertheless, the high mass-demanding photocatalyst preparation and the major role of the solvent in determining the process waste severely impair the photoredox protocol, which is carried out under diluted conditions (0.1 M vs 0.25 M). Advantages of the Lei's protocol are the use of not chlorinated β-ketoester **12** and the absence of heavy metals, however, the catalytic iodine[60] is classified as toxic (red flag), the reaction requires heating for 20 hours (60 °C, green flag) and, most importantly, DCE[44] is severely harmful (dark red flag).

In the same year, the Lei's research group also published the synthesis of dihydrofurans from β-ketocarbonyl compounds and olefins catalyzed by $CuCl_2$ (Scheme 10).[61]

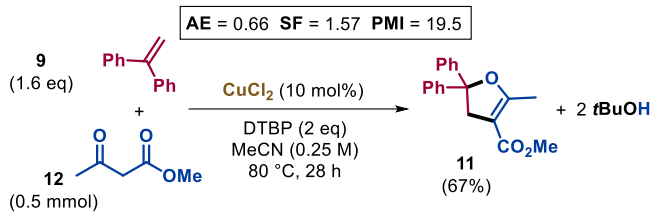

Scheme 10. Copper-catalyzed synthesis of 2,3-dihydrofuran **11** proposed by Lei in 2015.

The AE (0.66) is slightly better than the iodine-promoted reaction (0.51) and analogous to the photocatalytic approach (0.62). The SF (1.57) worsened because of the excess of olefin **9** and oxidant (DTBP), whose homolytic cleavage yields two *tert*-butyloxy radicals. Despite the unfavorable stoichiometric factor and the modest yield (67%), the PMI (19.5) is better than both photochemical and iodine-promoted protocols. The reaction waste consists of 86% acetonitrile[44] (yellow flag), which has a lower molecular weight and a significantly better health and environmental profile than DCE[17a,44] (Scheme 9). Solvent recovery would allow to reach PMI = 3.6, still higher than the photoredox process value (2.25). The catalyst $CuCl_2$ is less toxic than iodine; however, the toxicity of the oxidant DTBP[62] is remarkably higher (red flag) than that of TBPB, and it is used in excess. Lastly, a high temperature (80 °C, yellow flag) must be maintained for 28 h.

The last protocol that we describe was reported by Nishino in 2015 and exploits the traditional Mn(III)-promoted oxidation of β-dicarbonyl compounds (Scheme 11).[63] The SF is optimal (1) being all the reagents used in the exact stoichiometric proportion. The transformation is not catalytic; therefore the stoichiometric oxidant is quantitatively transformed, yielding a remarkable mass of by-products. As a consequence, the AE is rather low (0.35).

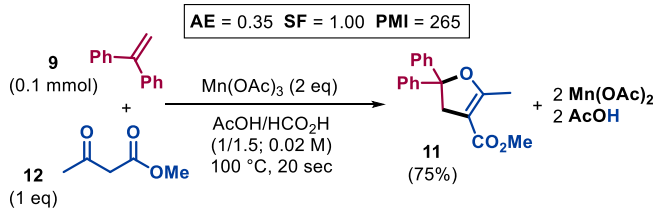

Scheme 11. Manganese-promoted synthesis of 2,3-dihydrofuran **11** proposed by Nishino in 2015.

The calculated PMI is burdensome (265), the highest one among the evaluated syntheses of dihydrofuran **11**. The reaction was carried out under very diluted conditions (0.02 M) leading to 99% of the process waste consisting of acidic solvents. Solvent recovery would greatly improve the PMI (reaching 3.8), but it would still be worse than the photocatalytic process (2.25). Advantages of this protocol are the reported high reaction rate (20 seconds) and the not toxic manganese-based stoichiometric oxidant and by-products (green flag). On the other hand, the major components of the reaction mixture, namely acetic acid[64] and formic acid,[65] are characterized by health concerns (yellow flags).

The comparison between the green chemistry metrics of the analyzed protocols for the synthesis of dihydrofuran **11** is summarized in Table 7.

Table 7. Comparison between the green chemistry metrics of the protocols for the synthesis of dihydrofuran **11**.[a]

	Scheme 8[55]	Scheme 9[59]	Scheme 10[61]	Scheme 11[63]
AE	0.62	0.51	0.66	0.35
SF	1.06	1.50	1.57	1.00
Yield [%]	77	61	67	75
PMI	37	33	19.5	265
PMI_{SR}	2.25	4.9	3.6	3.8
PMI_{G}	143	33	-	-
Time	24 h	20 h	28 h	20 s
Temp [°C]	rt	60	80	100

[a] PMI_{SR} = PMI with solvent recycled; PMI_{G} = PMI including the impact of the catalyst synthesis; Temp = reaction temperature; rt = room temperature; h = hours; s = seconds.

2.2.3 Decarboxylative Cross Coupling

Carboxylic acids are among the most abundant building blocks available for organic synthesis. Moreover they are widely found in naturally occurring feedstocks such as amino acids, fatty acids and sugar acids.[66] In addition to their conventional two-electron reactivity, they can also be employed as versatile reagents to form new C–C bonds through decarboxylative cross-coupling reactions.[67] In this context, carboxylic acids benefit from the widespread commercial availability and for being less toxic and/or more stable than the more reactive coupling partners, such as halides or organometallics.[66] In this regard, alkyl carboxylic acids can be used to generate alkyl radicals *via* single electron transfer (SET), involving the extrusion of CO_2. The preponderance of modern decarboxylative C–C bond formations employing alkyl radical intermediate relies on two different radical generation strategies.[66] The first strategy foresees the SET oxidation of the carboxylate ion ($E_{1/2}$ = +1.25 to +1.31 V vs SCE),[68] followed by the rapid decarboxylation of the carboxyl radical (k ≈ 10^9 s^{-1} at 20 °C),[69] that will generate the alkyl radical. The SET step can be mediated by a stoichiometric oxidant (e.g., $K_2S_2O_8$), high valent metal catalysts (e.g., Ag^{II}), excited photocatalysts (both metal-based or organic dyes), or an anode in electrosynthesis.[67] On the other hand, the second strategy relies on the SET reduction of the pre-activated carboxylic acid such as *N*-(acyloxy)phthalimide ester.[67a] Regarding the C–C bond forming step, nucleophilic alkyl radical intermediates can be used exploiting their innate radical reactivity, such as in the addition to electron-deficient π-systems,[70] or they can be merged with organometallic catalysts for the construction of new C–C bonds *via* reductive elimination

from the coordination sphere of a transition metal. In the latter case, the "metallaphotoredox" catalysis has proven to be a fruitful research area.[71]

2.2.3.1 Acyl Radicals Generation

Ketones are a crucial functional group in organic synthesis due to their ability to act as electrophiles in a wide array of bond-forming reactions. Moreover, diaryl ketones are a common structural moiety found in a broad range of bioactive natural products, pharmaceuticals, agrochemicals and functional materials.[72] A large number of methods have been developed for their preparations. Among these, radical acylation reactions *via* visible light photocatalysis have been widely studied in the past decades, as this methodology requires mild reaction conditions and expands the scope of organic molecules that can be acylated.[73] Among the most used acylating agents, α-keto acids have attracted much attention, due to their low cost, stability, easy preparation, and high reactivity.[74] The conversion of α-oxocarboxylic acids into acyl radicals can be achieved from the corresponding carboxylate by photocatalytic oxidation and subsequent decarboxylation.[75] Both metal-based photocatalysts[76] (e.g $[Ru(phen)_3]^{2+}$, $[Ir\{dF(CF_3)ppy\}_2(dtbbpy)]^+$) and organic dyes[77] (e.g Eosin Y, $MesAcr^+$) have been employed to promote this transformation. In this context, we selected three different reactions that exploit the decarboxylative arylation of α-oxo acids, aiming to evaluate the sustainability of the process when promoted by a metal-based photocatalyst, an organic dye, or a catalyst not requiring light.

In 2015, MacMillan and co-workers published a seminal work describing the first radical decarboxylative coupling of α-oxo acids and aryl halides, promoted by a metal-based photocatalyst and a transition-metal catalyst synergistically working[76b] (Scheme 12).

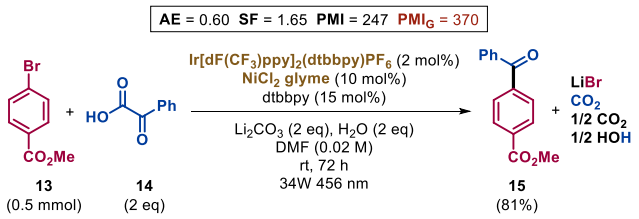

Scheme 12. Photocatalytic synthesis of product **15** proposed by MacMillan in 2015.

We analyzed the green chemistry metrics of the reaction carried out on methyl 4-bromobenzoate **13** and 2-oxo-2-phenylacetic acid **14** in the presence of $[Ir\{dF(CF_3)ppy\}_2(dtbbpy)]^+$ (**C**) and a catalytic Ni complex. The AE of the process resulted 0.60, significantly limited by the inevitable generation of by-products (LiBr, CO_2 and H_2O). The stoichiometric factor (SF = 1.65, 1/SF = 0.61) is also penalized by the use of excess of acid and base (2 equivalents for both) (Figure 12).

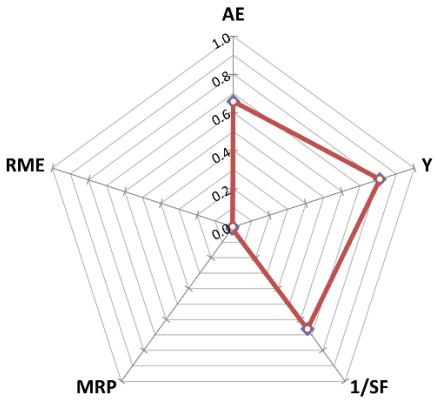

Figure 12. Performance pentagon for the photocatalytic synthesis proposed by MacMillan in 2015.

Despite the high yield (81%), PMI shows that 247 g of materials are required to produce 1 g of product **15**, effectively generating 246 g of waste. While this number is significant, upon careful examination of reaction waste, it can be observed that only 1% of the total waste mass consists of reagent excess, by-products or catalysts, while the remaining 99% derives from the solvent (Figure 13).

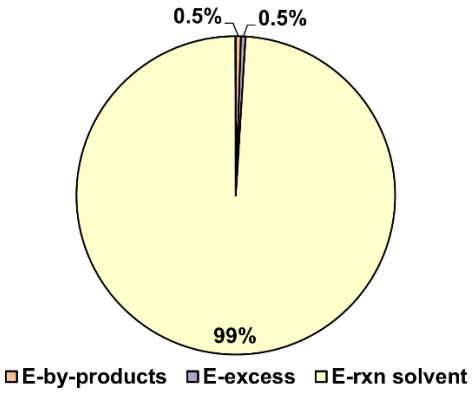

Figure 13. Distribution of the total waste of the MacMillan's synthesis of **15**.

Once again, the solvent plays the major role in the reaction waste. Indeed, if the solvent was recycled, the process efficiency could improve approximately 64 times (PMI = 3.9 vs 247). Concerning the reaction medium, the authors proposed *N*, *N*-dimethylformamide (DMF)[78] as the best one. However, like its parent DMA, it is toxic and it is classified as an hazardous solvent (red flag) according to the widely accepted solvent sustainability guides.[17a,36] Concerning the catalytic system two transition metal-based complexes are used. The photocatalyst ($[Ir\{dF(CF_3)ppy\}_2(dtbbpy)]PF_6$, **C**) is based on one of the rarest element on earth[79] (red flag) making the scalability of the process particularly challenging in terms of costs. On the other hand, even if nickel is more abundant[80] (yellow flag), the catalyst precursor ($NiCl_2$ glyme) is toxic[81] (red flag) and this can limit large-scale applications. Moreover, the nickel catalyst also requires a ligand (dtbbpy) to catalyze the formation of the product. Even if it is not toxic,[82] its use increases the total waste mass.

The same product **15** can also be obtained *via* a similar photoredox protocol involving an organic dye instead of a metal-based photocatalyst. This protocol has been reported by Li and co-workers in 2020[83] (Scheme 13).

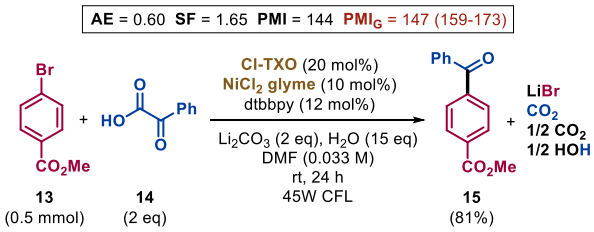

Scheme 13. Photocatalytic synthesis of product **15** proposed by Li in 2020.

Since this protocol is analogous to the one reported by MacMillan in terms of starting materials, co-catalyst, and base, the AE and the SF factors are exactly the same (AE = 0.60, SF = 1.65). In this case, an improvement of the process efficiency has been achieved by increasing the reaction concentration (0.033 M vs 0.020 M) resulting in a substantial reduction of the PMI (144 vs 247). However, the solvent still results to be the major source of waste, being the 98% of the total waste mass (Figure 14). The remaining 2% is composed by the unavoidable by-products, excess of reagents and catalysts. Regarding the catalytic system, the substitution of the iridium-based photocatalyst with an organic dye is favorable, not only due to the cost and scarce availability of the first, but also because the molecular weight of the organic dye is lower. In this particular case, 20 mol% of the organic photocatalyst is used (10 times more than the MacMillan protocol), but the catalyst waste remains the same as before (0.17% vs 0.18%).

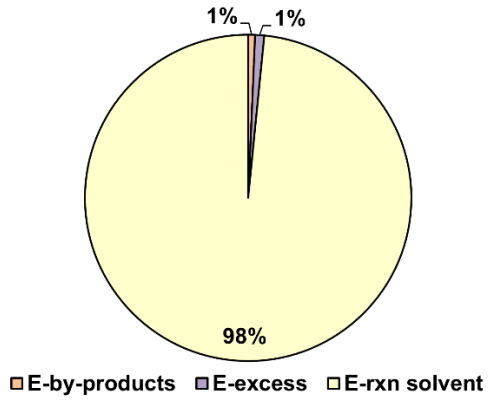

Figure 14. Distribution of the total waste of the Li's synthesis of **15**.

Once analyzed two photocatalytic protocols for the decarboxylative cross-coupling *via* acyl radical formation, we turned our attention to a methodology that does not rely on light, but it is able to provide the same product **15**. The procedure proposed by Ranu *et al.* in 2018[84] performs the decarboxylation of 2-oxo-2-phenylacetic acid **14** using a stoichiometric oxidant and the formed acyl radical is coupled with a diazonium salt (**16**) through the use of a palladium catalyst (Scheme 14).

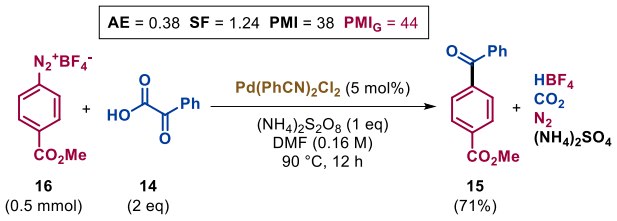

Scheme 14. Thermal synthesis of product **15** proposed by Ranu in 2018.

The AE of this protocol is significantly worse than those of the photoredox strategies (0.38 vs 0.60), primarily because of the stoichiometric quantity of oxidant. On the other hand, the SF (1.24) results to be the lowest, since only the ketoacid **14** is used in excess (2 equivalents). Despite the lower yield (71%), the PMI (38) is better than the photocatalytic approaches thanks to the higher concentration (0.16 vs 0.033 or 0.02 M). The solvent recovery would enable a remarkable decrease of PMI (4.7), still higher than the corresponding light-promoted reactions. Regarding the total waste mass, 90% comes from the solvent, while the remaining 10% is primarily derived from the by-products and the excess reagents. Concerning process safety, it must be noted that both the reaction solvent (DMF)[78], the stoichiometric oxidant[85] and the Pd-based catalyst[86] are significantly toxic (red flags). Moreover, the employed catalyst is based on an expensive and scarcely available element[87] (yellow flag). Even if the reaction doesn't need to be irradiated in order to proceed, the temperature has to be increased up to 90 °C and maintained for 12 hours (yellow flag). In this specific case, we examined also the straightforward synthesis of the palladium catalyst,[88] finding that the PMI for its preparation is rather low (PMI_{CAT} = 82), making the global PMI the lowest in the series.
The green chemistry metrics analysis for the acyl radical mediated synthesis of **15** is summarized in Table 8.

Table 8. Summary of the green metrics analysis for synthesis of diaryl ketone **15** *via* acyl radical formation.[a]

	Scheme 12[76b].	Scheme 13[83]	Scheme 14[84].
AE	0.60	0.60	0.38
SF	1.65	1.65	1.24
Yield [%]	81	85	71
PMI	247	144	38
PMI_{SR}	3.9	3.5	4.7
PMI_G	374	159-173	44
Time	72 h	24 h	12 h
Temp [°C]	37	rt	90

[a] PMI_{SR} = PMI with solvent recycled; PMI_G = PMI including the impact of the catalyst synthesis; Temp = reaction temperature; rt = room temperature; h = hours.

2.2.3.2 α-Aminoalkyl Radicals *via* Amino Acids Decarboxylation

Allylic amines are among the most important and highly versatile building blocks for organic synthesis. In particular, they are attractive for their role as pharmacophores in numerous building blocks, and for their versatility as intermediates in the production of medicinal agents.[89] Indeed, in last decades, numerous methods have been reported for their preparation.[90] Among them, various photocatalytic processes employing the decarboxylation of natural amino acids have attracted much attention. In this section, we will use green chemistry metrics to evaluate the sustainability of some photoredox protocols that allow the preparation of allyl amines *via* decarboxylation of natural α-amino acids.

In 2014, MacMillan and co-workers published the first example of photoredox α-vinylation of α-amino acids that works through the formation of an α-amino radical (Scheme 15).[91] This reaction is carried out on *L*-proline **17** and (*E*)-(2-(phenylsulfonyl)vinyl)benzene **18** in the presence of $[Ir(ppy)_2(dtbbpy)]PF_6$ (**H**) as the photocatalyst.

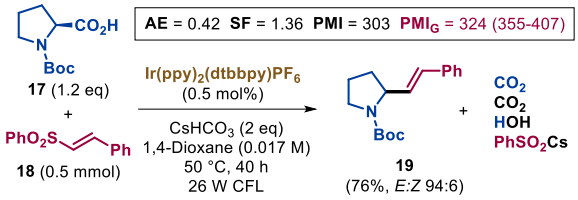

Scheme 15. Photocatalytic synthesis of product **19** proposed by MacMillan in 2014.

The green chemistry metrics calculation shows an AE of 0.42 (Figure 15) significantly limited by the leaving groups in the starting materials. In particular, the molecular weight of cesium benzenesulfinate (274.07 g/mol), similar to that of the product (273.38 g/mol), and its unavoidable formation lower the AE value. On the other hand, the stoichiometric factor (SF =1.36, 1/SF = 0.73, Figure 15) is sufficiently low. Only the base is used in a substantial excess (2 equivalents), while only a slight excess of *L*-proline is required. The PMI was found to be 303, indicating that 302 g of waste are produced for every gram of product **19**. The major source of waste (99% of the total) is once again the solvent. In fact, the process efficiency could improve approximately 70 times by recycling the reaction medium (PMI = 4.3 vs 303).

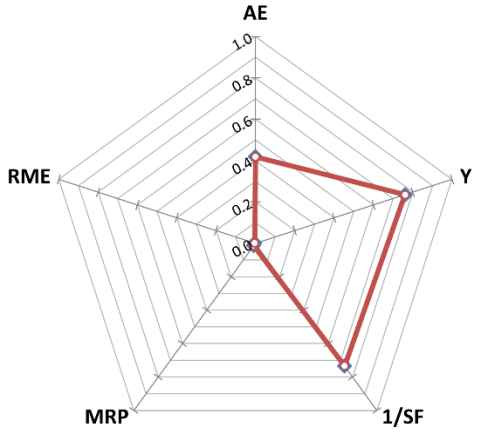

Figure 15. Performance pentagon for the photocatalytic synthesis of **19** proposed by MacMillan in 2014.

Since the solvent is the main source of waste, its hazardous nature significantly affects the overall sustainability of the process. In this case, the best solvent proposed was 1,4-dioxane, that is toxic[92] and classified as hazardous medium especially because of its safety score[17a] (red flag). Regarding the catalyst, as already mentioned, iridium is expensive and rare (red flag). Finally, it's noteworthy that the reaction not only requires light, but also a high temperature (50 °C, green flag) to be maintained for an extended period (40 h).

Recently, Panda *et al.*[93] proposed a protocol similar to the MacMillan's procedure for the preparation of product **19**, which employs the organic dye 4CzIPN (**E**) instead of the iridium-based catalyst (Scheme 16).

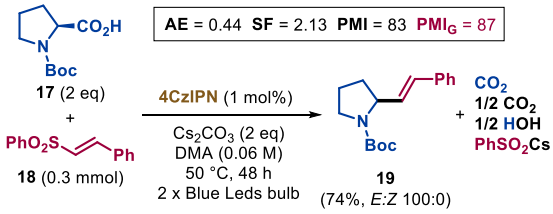

Scheme 16. Photocatalytic synthesis of product **19** proposed by Panda in 2022.

Since the used starting materials match those used by MacMillan, the AE of the process is very similar to the previous one (0.44 vs 0.42). On the other hand, due to the substantial excess (2 equivalents) of both the base and *L*-proline, the SF was worse (2.13 vs 1.36). The increased concentration (0.06 M vs 0.017 M) results in a notable improvement in reaction efficiency, reducing the PMI to 83 and, consequently, the mass of produced waste. As expected, the solvent (DMA, red flag) still proves to be the major source of waste, accounting for 93% of the total waste mass (Figure 16). Particularly noteworthy is the improvement in process efficiency that could be achieved if solvent recycling is considered. The new value of PMI would be 6.5, almost 1.5 times higher than the previous protocol (4.3). In fact, the excess of both base and amino acid increases the portion of waste derived from reagent excesses in this approach (4%, Figure 16).

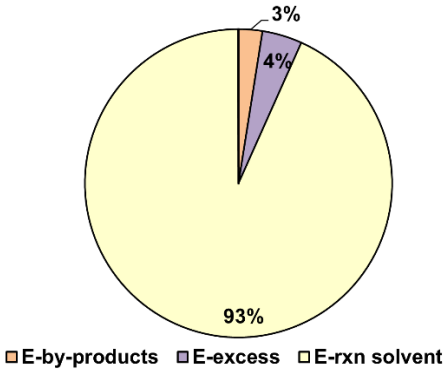

Figure 16. Distribution of the total waste of the Panda's synthesis of **19**.

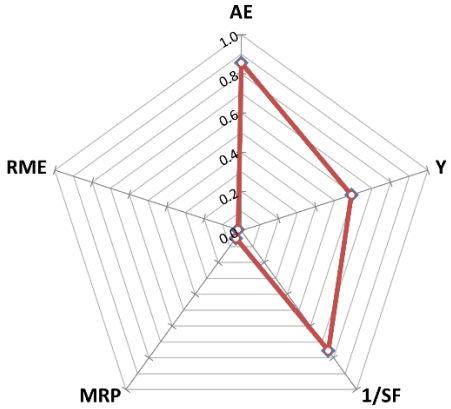

Figure 17. Performance pentagon for the photocatalytic synthesis of **19** proposed by Wu in 2018.

The use of an organic dye allows to avoid the concerns related to a rare element. Also in this case, 50 °C (green flag) have to be maintained for an extended period (48 h). It's worth mentioning that the same authors also proposed an alternative but similar set of conditions allowing to obtain product **19** with the opposite double bond configuration. This second protocol employs 1,4-dioxane (0.075 M) as solvent (red flag), and the reaction proceeds at room temperature for 48 h. In terms of green metrics, the values of AE and SF remained unchanged, while the PMI (74) decreased due to the higher concentration.

In 2018, Wu and co-workers proposed a different photocatalytic method for the preparation of product **19** (Scheme 17).[94]

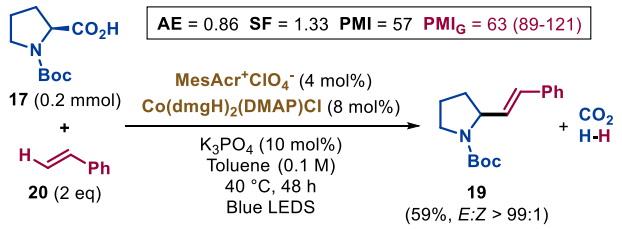

Scheme 17. Photocatalytic synthesis of product **19** proposed by Wu in 2018.

This protocol is able to form the same bond as the previous strategies, but it exploits a different mechanism enabled by a synergistic catalysis between an organic dye ($MesAcrClO_4$, **K**) and a cobalt co-catalyst. The AE (Figure 17) is almost two times higher than the previous ones (0.86 vs 0.42 and 0.44), indicating that only half of the by-products are produced. Indeed, (*E*)-(2-(phenylsulfonyl)vinyl)benzene **18** has been substituted with styrene **20** as a vinyl synthon, avoiding the production of cesium benzenesulfinate as by-product. Moreover, the SF (1.33, 1/SF = 0.75, Figure 17) is almost two times lower than Panda's protocol[93] and almost the same as the MacMillan's one[91] (Scheme 17 vs Schemes 15 and 16). The low SF is due to the styrene **20** being the only reagent used in excess. On the other hand, it's worth mentioning that the yield is lower in this process (Figure 17) compared to the previous ones (59% vs 76% and 74%).

In terms of PMI, this protocol has the lowest value. In particular, 57 g of materials are needed to produce 1 g of product. The generated waste is primarily composed (96%, Figure 18) by the solvent, while the remaining 4% consists of by-products, excess reagents and catalysts. If a solvent recycling is considered, a reduction in PMI of 18 times can be achieved (3.1 vs 57).

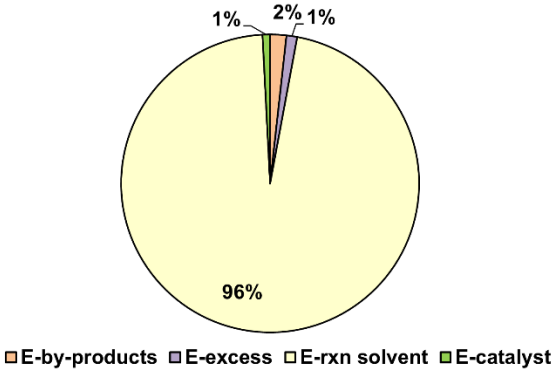

Figure 18. Distribution of the total waste of the Wu's synthesis of **19**.

Regarding the reaction medium, the authors proposed toluene as the best one. However, it is toxic[95] and classified as problematic solvent[17a] (yellow flag). Regarding the catalytic system, in the Wu's vinylation, the reaction is promoted by $MesAcrClO_4$ and $Co(dmgH)_2(DMAP)Cl$ that are not harmful for the human health.[96] Moreover, cobalt is not critical in terms of earth-abundance[80] (yellow flag).

An alternative method for generating the α-amino radical from an amino acid through photocatalytic decarboxylation involves the use of its phthalimide ester derivative. In this case, the reaction mechanism differs from the previous approaches, leading to a reductive decarboxylation process instead of an oxidative one. In 2017, Wang and co-workers[97] reported the synthesis of product **19** through a dual decarboxylation that involves the phthalimide ester **21** of *L*-proline (Scheme 18).

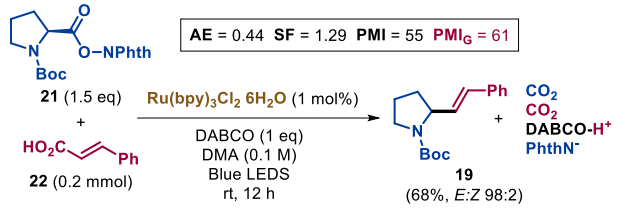

Scheme 18. Photocatalytic synthesis of product **19** proposed by Wang in 2017.

We analyzed the green chemistry metrics of this reaction to compare the use of phthalimide ester with free carboxylic acid for the synthesis of product **19**. The AE resulted 0.44, mainly due to the unavoidable generation of the phthalimide anion and the DABCO-H$^+$ counterion. It is noteworthy the similarity between the AE of this protocol and those of MacMillan's[91] and Panda's[93] procedures, meaning that the loss of mass caused by the phthalimide anion is counterbalanced by the generation of the benzenesulfinate salt in the previous protocols. The SF (1.29) is quite low, as only reagent **21** is used in a slight excess. The calculated PMI is similar to the Wu's[94] protocol (55 vs 57). In fact, also in this case, the generated waste is composed of solvent (96%), by-products (4%) and excess reagents (2%). The solvent recycling could decrease the PMI down to 4.4. It's worth mentioning that the lower values of PMI in the last two protocols is due to the reduced amount of solvent used (0.1 vs 0.06 and 0.017 M). Regarding process safety, as mentioned earlier, DMA is toxic[98] and it has been classified as hazardous solvent[17a] (red flag). Concerning the metal-based photocatalyst, ruthenium is a rare element (red flag). In conclusion, it is important to emphasize that the green metrics of this process are comparable to or even better (in terms of PMI) than those previously reported, however, reagent **21** must be prepared starting from *L*-proline **17**, which is the starting material in the other protocols.

Once analyzed four different photocatalytic protocols for the α-vinylation of amino acids, we turned our attention to a not light-promoted methodology able to provide the same product **19**. The procedure proposed by Lu *et al.*[99] in 2001 yields the same product starting from *N*-Boc-pirrolidine **23** employing a different mechanism (Scheme 19).

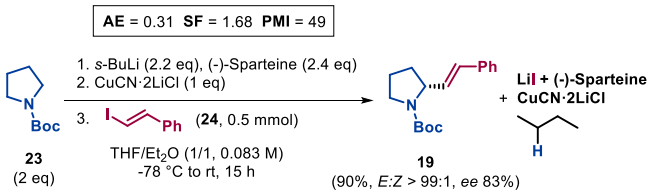

Scheme 19. Synthesis of product **19** proposed by Lu in 2001.

The AE (0.31, Figure 19) is lower than those of the photoredox strategies due to the use of additives (CuCN·2LiCl and (−)-sparteine) that are not consumed during the reaction and inevitably end up in the by-products. Moreover, additives are also used in excess affecting the SF (1.68, Figure 19) which results higher than the values of MacMillan (1.36),[91] Wu (1.33),[94] and Wang (1.29),[97] but lower than Panda's value (2.13).[93]

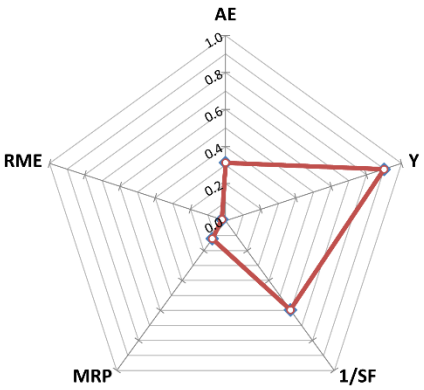

Figure 19. Performance pentagon for the synthesis of **19** proposed by Lu in 2001.

On the other hand, the PMI (49) is better than the photocatalytic processes due to the higher yield (90%, Figure 19) and concentration (0.08 M). It is worth mentioning that, if a medium recycling is considered, the PMI would reach 6.0, higher than all the previously analyzed photocatalytic processes except for the Panda's one.[93] This value of PMI points out that, in this protocol, a remarkable part of the waste mass (10%) comes from excess of reagents and by-products (Figure 20).

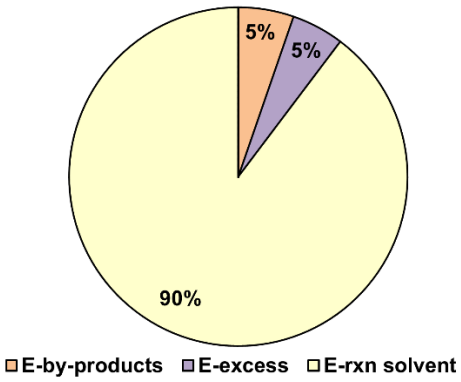

Figure 20. Distribution of the total waste of the Lu's synthesis of **19**.

Concerning the process safety, it must be noted that *sec*-butyllithium[100] and the co-product butane[101] are dangerous substances (red flag). Moreover both the solvents (Et$_2$O,[102] dark red flag; THF,[103] red flag) and CuCN[104] (yellow flag) are significantly toxic. The absence of catalyst might be advantageous for the process sustainability, partly counterbalanced by the cryogenic conditions (−78 °C, red flag) to be maintained for 3 hours, and the use of supra-stoichiometric amount of reagents. It is important to stress, however, that in this case a primary goal of the synthetic protocols is the stereoselective preparation of product **19**, which requires very low temperatures and high molecular weight ligands. The green chemistry metrics analysis for the synthesis of α-vinyl pyrrolidine **19** is summarized in Table 9.

Table 9. Summary of the green metrics analysis for the construction of α-vinyl pyrrolidine **19**.[a]

	Scheme 15[91]	Scheme 16[93]	Scheme 17[94]	Scheme 18[97]	Scheme 19[99]
AE	0.42	0.44	0.86	0.44	0.31
SF	1.36	2.13	1.33	1.29	1.68
Yield [%]	76	74	59	68	90
PMI	303	83	57	55	49
PMI_{SR}	4.3	6.5	3.1	4.4	6.0
PMI_G	355-407	87	89-121	61	49
Time	40 h	48 h	24 h	12 h	15 h
Temp [°C]	50	50	40	rt	−78 to rt

[a] PMI_{SR} = PMI with solvent recycled; PMI_G = PMI including the impact of the catalyst synthesis; Temp = reaction temperature; rt = room temperature; h = hours.

3. Summary and Outlook

In this Review, the sustainability of photocatalytic processes in synthetic chemistry has been critically evaluated using mass-based metrics. The analysis encompassed the synthesis of common photocatalysts and various photoredox catalytic reactions, comparing their efficiency with more traditional processes in the absence of light. Several key conclusions can be summarized as follows:

1. The synthesis of photocatalysts revealed several significant sustainability issues. Most of the examined procedures have high PMI values, primarily due to the extensive use of solvents employed in the work-up and purification stages. Moreover, all the preparations of metal-based photocatalysts are energy-intensive reactions, using rare and costly elements.

2. The waste generated during a photocatalyst synthesis was shown to significantly influence the overall efficiency of a catalytic protocol. Even when used in small amounts (mol%), catalysts with high PMI values could contribute substantially to the overall waste of a catalytic process (PMI_G). Therefore, the impact of photocatalyst preparation on the overall sustainability of a catalytic protocol should not be underestimated.

3. As expected, we found that solvents played a major role in the waste generated, both during the synthesis of photocatalysts and the catalytic protocols. Work-up and purification stages were identified as the primary contributors to waste, with organic solvents playing a major role. Therefore, a careful choice of solvents, including an analysis of their toxicological profile, and purification procedures are the key factors in determining the final overall sustainability of catalytic processes, far more important than the choice of the protocol itself.

4. Photocatalytic reactions are mostly carried out under very diluted conditions to avoid light penetration issues. It can greatly damage the process sustainability. However, in several cases, higher concentrations would be well tolerated. Moreover, alternative solutions (for instance flow photocatalysis) are available, that could allow to reduce the waste production without depressing the process productivity.

5. The replacement of a metal-based photocatalyst with an organic dye is generally advantageous for the sustainability profile of a catalytic protocol, not only due to the higher costs of rare metals, but also thanks to the greater sustainability of the organic dyes preparations and to their lower molecular weight.

In conclusion, we found that the sustainability of photoredox catalytic procedures cannot be solely ascribed to the use of light or to catalytic efficiency, and we believe that the notion of green chemistry in the field of photocatalysis may sometimes be overstated. Sustainability assessments should consider in detail the entire protocol, from catalyst preparation to work-up and purification stages, considering both quantitative and qualitative factors. While photoredox catalysis offers the potential for more sustainable chemical transformations, and in some cases allows the straightforward construction of otherwise difficult-to-obtain molecular architectures, careful consideration of the specific reaction conditions and the broader environmental impact is essential to exploit its full potential in the development of environmentally friendly and sustainable chemical processes. Organic photocatalytic processes are regarded as promising technologies for addressing sustainability and energy-related challenges associated with traditional synthetic transformations. However, despite significant efforts has been devoted to the development of new photocatalytic transformation, the practical applications of organic photocatalysis on a larger scale for future industrial developments remain limited. To move from laboratory research to large-scale processes, it is crucial to reassess the synthesis of current photocatalysts or to design new high-performance photocatalysts using safe, cost-effective, and environmentally sustainable synthetic pathways, paying particular attention to the use of organic solvents and purification strategies. An aspect that should be further explored is the impact of the nature of the light source on the process sustainability. In fact, photons wavelength and intensity could play an important role enabling a fine tuning of the photocatalyst reactivity and of the reaction selectivity.[105] Currently, few details are provided in the literature supporting the choice of a peculiar light source, which, therefore, seems to be not optimized to achieve maximum efficiency, selectivity and sustainability.

Keywords: Photoredox catalysis • Sustainability • Green metrics • Solvents • Visible light

[1] D. A. Nicewicz, D. W. C. MacMillan, *Science* **2008**, *322*, 77–80.

[2] M. A. Ischay, M. E. Anzovino, J. Du, T. P. Yoon, *J. Am. Chem. Soc.* **2008**, *130*, 12886–12887.

[3] J. M. R. Narayanam, J. W. Tucker, C. R. J. Stephenson, *J. Am. Chem. Soc.* **2009**, *131*, 8756–8757.

[4] a) Y. Markushyna, A. Savateev, *Eur J Org Chem* **2022**, *2022*, e202200026; b) M. V. Bobo, J. J. Kuchta, A. K. Vannucci, *Org. Biomol. Chem.* **2021**, *19*, 4816–4834; c) S. G. E. Amos, M. Garreau, L. Buzzetti, J. Waser, *Beilstein J. Org. Chem.* **2020**, *16*, 1163–1187; d) B. König, *Eur J Org Chem* **2017**, *2017*, 1979–1981; e) M. H. Shaw, J. Twilton, D. W. C. MacMillan, *J. Org. Chem.* **2016**, *81*, 6898–6926; f) N. A. Romero, D. A. Nicewicz, *Chem. Rev.* **2016**, *116*, 10075–10166. Progress in organic photocatalytic transformations has been recently addressed in a special issue of *The Journal of Organic Chemistry*: g) M. Akita, P. Ceroni, C. R. J. Stephenson, G. Masson *J. Org. Chem.* **2023**, *88*, 6281–6283.

[5] a) G. Ciamician, P. Silber, *Ber. Dtsch. Chem. Ges.* **1908**, *41*, 1928–1935; b) G. Ciamician, *Science* **1912**, *36*, 385–394.

[6] G. E. M. Crisenza, P. Melchiorre, *Nat. Commun.* **2020**, *11*, 803.

[7] L. Marzo, S. K. Pagire, O. Reiser, B. König, *Angew. Chem. Int. Ed.* **2018**, *57*, 10034–10072.

[8] a) S. A. Espinosa, A. Bala, P. Fullana-i-Palmer, *Green Chem.* **2022**, *24*, 7751–7762; b) H. B. Rose, B. Kosjek, B. M. Armstrong, S. A. Robaire, *Curr. Res. Green Sustain. Chem.* **2022**, *5*, 100324.

[9] a) P.-M. Jacob, P. Yamin, C. Perez-Storey, M. Hopgood, A. A. Lapkin, *Green Chem.* **2017**, *19*, 140–152; b) C. R. McElroy, A. Constantinou, L. C. Jones, L. Summerton, J. H. Clark, *Green Chem.* **2015**, *17*, 3111–3121.

[10] A. Antenucci, S. Dughera, P. Renzi, *ChemSusChem* **2021**, *14*, 2785–2853.

[11] Anastas, P. T., Warner, J. C., *Green, Chemistry, Theory and Practice*, Oxford University Press, New York, **1998**.

[12] B. M. Trost, *Science*, **1991**, *254*, 1471–1477.

[13] R. A. Sheldon, *Chem. Ind.*, **1992**, 903–906.

[14] a) D. J. C. Constable, A. D. Curzons, V. L. Cunningham, *Green Chem.* **2002**, *4*, 521–527; b) R. A. Sheldon, *ACS Sustainable Chem. Eng.* **2018**, *6*, 32–48.

[15] a) A. D. Curzons, D. J. C. Constable, D. N. Mortimer, V. L. Cunningham, *Green Chem.* **2001**, *3*, 1–6; b) J. Andraos, *Org. Process Res. Dev.* **2005**, *9*, 149–163.

[16] J. Andraos, *ACS Sustainable Chem. Eng.* **2018**, *6*, 3206–3214.

[17] a) D. Prat, A. Wells, J. Hayler, H. Sneddon, C. R. McElroy, S. Abou-Shehada, P. J. Dunn, *Green Chem.* **2016**, *18*, 288–296; b) D. Prat, J. Hayler, A. Wells, *Green Chem.* **2014**, *16*, 4546–4551.

[18] K. A. Teegardinm J. D. Weaver, *Org. Synth.* **2018**, *95*, 29–45.

[19] M. S. Oderinde, J. W. Johannes, *Org. Synth.* **2017**, *94*, 77–92.

[20] S. D. Lies, S. Lin, T. P. Yoon, *Org. Synth.* **2016**, *93*, 178–199.

[21] S. M. Engle, T. R. Kirkner, C. B. Kelly, *Org. Synth.* **2019**, *96*, 455–473.

[22] J. Andraos, *Green Process. Synth.* **2019**, *8*, 324–336.

[23] K. Nakanishi, G. J. T. Cooper, L. J. Points, L. G. Bloor, M. Ohba, L. Cronin, *Angew. Chem. Int. Ed.* **2018**, *57*, 13066–13070.

[24] N. R. Patel, C. B. Kelly, M. Jouffroy, G. A. Molander, *Org. Lett.* **2016**, *18*, 764–767.

[25] a) S. Sprouse, K. A. King, P. J. Spellane, R. J. Watts, *J. Am. Chem. Soc.* **1984**, *106*, 6647–6653; b) A. D. de Bruijn, G. Roelfes, *Chem. Eur. J.* **2018**, *24*, 11314–11318.

[26] M.-J. Yi, T.-F. Xiao, W.-H. Li, Y.-F. Zhang, P.-J. Yan, B. Zhang, P.-F. Xu, G.-Q. Xu, *Chem. Commun.* **2021**, *57*, 13158–13161.

[27] R. Ding, H. Chen, Y.-L. Xu, H.-T. Tang, Y.-Y. Chen, Y.-M. Pan, *Adv. Synth. Catal.* **2019**, *361*, 3656–3660.

[28] X.-Y. Huang, R. Ding, Z.-Y. Mo, Y.-L. Xu, H.-T. Tang, H.-S. Wang, Y.-Y. Chen, Y.-M. Pan, *Org. Lett.* **2018**, *20*, 4819–4823.

[29] G. Benkovics, D. Afonso, A. Darcsi, S. Béni, S. Conoci, É. Fenyvesi, L. Szente, M. Malanga, S. Sortino, *Beilstein J. Org. Chem.* **2017**, *13*, 543–551.

[30] T. A. Schmidt, C. Sparr, *Angew. Chem. Int. Ed.* **2021**, *60*, 23911–23916.

[31] a) K. Nakajima, Y. Miyake, Y. Nishibayashi, *Acc. Chem. Res.* **2016**, *49*, 1946–1956; b) Y.-Q. Zou, W.-J. Xiao in *Visible Light Photocatalysis in Organic Chemistry, Chapter 4* (Eds.: C. R. J. Stephenson, T. P. Yoon, D. W. C. MacMillan), Wiley-VCH Verlag GmbH & Co. Weinheim, Germany, **2018**, pp. 93–127.

[32] a) K. G. Roberts, L. J. Janke, Y. Zhao, A. Seth, J. Ma, D. Finkelstein, S. Smith, K. Ebata, B. B. Tuch, S. P. Hunger, C. G. Mullighan, *Blood* **2018**, *132*, 861–865; b) S. L. Lowe, C. J. Wong, J. Witcher, C. R. Gonzales, G. L. Dickinson, R. L. Bell, L. Rorick-Kehn, M. Weller, R. R. Stoltz, J. Royalty, S. Tauscher-Wisniewski, *J. Clin. Pharmacol.* **2014**, *54*, 968–978.

[33] N. A. McGrath, M. Brichacek, J. T. Njardarson, *J. Chem. Educ.* **2010**, *87*, 1348–1349.

[34] A. McNally, C. K. Prier, D. W. C. MacMillan, *Science* **2011**, *334*, 1114–1117.

[35] https://echa.europa.eu/it/substance-information/-/substanceinfo/100.004.389.

[36] a) C. M. Alder, J. D. Hayler, R. K. Henderson, A. M. Redman, L. Shukla, L. E. Shuster, H. F. Sneddon, *Green Chem.* **2016**, *18*, 3879–3890; b) V. Hessel, N. Tran, R. Asrami, Q. D. Tran, N. Van Duc Long, M. Escribà-Gelonch, J. O. Tejada, S. Linke, K. Sundmacher, *Green Chem.* **2022**, *24*, 410–437; c) D. Prat, J. Hayler, A. Wells, *Green Chem* **2014**, *16*, 4546–4551.

[37] https://echa.europa.eu/it/substance-information/-/substanceinfo/100.005.091.

[38] a) J. D. Hayler, D. K. Leahy, E. M. Simmons, *Organometallics* **2019**, *38*, 36–46; b) T. Watari, K. Nansai, K. Nakajima, *Resour. Conserv. Recycl.* **2021**, *164*, 105107; c) N. Hoffmann, *ChemSusChem* **2012**, *5*, 352–371.

[39] a) C. T. J. Ferguson, K. A. I. Zhang, *ACS Catal.* **2021**, *11*, 9547–9560; b) A. A. Yakushev, A. S. Abel, A. D. Averin, I. P. Beletskaya, A. V. Cheprakov, I. S. Ziankou, L. Bonneviot, A. Bessmertnykh-Lemeune, *Coord. Chem. Rev.* **2022**, *458*, 214331; c) A. Abramov, S. Bonardd, R. Pérez-Ruiz, D. Díaz Díaz, *Adv. Synth. Catal.* **2022**, *364*, 2–17.

[40] A. Quintavalla, D. Carboni, C. Sepe, L. Mummolo, N. Zaccheroni, M. Lombardo, *Adv. Synth. Catal.* **2023**, *365*, 252–262.

[41] https://echa.europa.eu/it/substance-information/-/substanceinfo/100.020.399.

[42] https://echa.europa.eu/it/substance-information/-/substanceinfo/100.009.531.

[43] Z. Luo, Y. Pan, Z. Yao, J. Yang, X. Zhang, X. Liu, L. Xu, Q.-H. Fan, *Green Chem.* **2021**, *23*, 5205–5211.

[44] https://echa.europa.eu/it/substance-information/-/substanceinfo/100.000.760.

[45] a) Z. Rezaei, H. Firouzabadi, N. Iranpour, A. Ghaderi, M. R. Jafari, A. A. Jafari, *Eur. J. Med. Chem.* **2009**, *44*, 4266–4275; b) A. Mucha, P. Kafarski, Ł. Berlicki, *J. Med. Chem.* **2011**, *54*, 5955–5980.

[46] L. Niu, S. Wang, J. Liu, H. Yi, X.-A. Liang, T. Liu, A. Lei, *Chem. Commun.* **2018**, *54*, 1659–1662.

[47] https://echa.europa.eu/it/substance-information/-/substanceinfo/100.003.145.

[48] M.-J. Yi, T.-F. Xiao, W.-H. Li, Y.-F. Zhang, P.-J. Yan, B. Zhang, P.-F. Xu, G.-Q. Xu, *Chem. Commun.* **2021**, *57*, 13158–13161.

[49] https://echa.europa.eu/it/substance-information/-/substanceinfo/100.000.603.

[50] W. Han, P. Mayer, A. R. Ofial, *Adv. Synth. Catal.* **2010**, *352*, 1667–1676.

[51] https://echa.europa.eu/it/substance-information/-/substanceinfo/100.000.599.

[52] https://echa.europa.eu/it/substance-information/-/substanceinfo/100.000.833.

[53] a) S. P. Pitre, N. A. Weires, L. E. Overman, *J. Am. Chem. Soc.* **2019**, *141*, 2800–2813; b) W.-T. Zhao, W. Shu, *Sci. Adv.* **2023**, *9*, eadg9898; c) Z. Chen, M.-Y. Rong, J. Nie, X.-F. Zhu, B.-F. Shi, J.-A. Ma, *Chem. Soc. Rev.* **2019**, *48*, 4921–4942.

[54] C.-Y. Huang, J. Li, C.-J. Li, *Chem. Sci.* **2022**, *13*, 5465–5504.

[55] A. Quintavalla, R. Veronesi, D. Carboni, A. Martinelli, N. Zaccheroni, L. Mummolo, M. Lombardo, *Adv. Synth. Catal.* **2021**, *363*, 3267–3282.

[56] a) S. Sari, M. Yilmaz, *Med. Chem. Res.* **2020**, *29*, 1804–1818; b) H. A. Oketch-Rabah, E. Lemmich, S. F. Dossaji, T. G. Theander, C. E. Olsen, C. Cornett, A. Kharazmi, S. B. Christensen, *J. Nat. Prod.* **1997**, *60*, 458–461.

[57] Z. Chen, A. Zhang, H. Xiao, F. Huo, Z. Zhen, X. Liu, S. Bo, *Dyes Pigm.* **2020**, *173*, 107876.

[58] a) A. Romero-Arenas, V. Hornillos, J. Iglesias-Sigüenza, R. Fernández, J. López-Serrano, A. Ros, J. M. Lassaletta, *J. Am. Chem. Soc.* **2020**, *142*, 2628–2639; b) J. D. Feist, Y. Xia, *J. Am. Chem. Soc.* **2020**, *142*, 1186–1189.

[59] S. Tang, K. Liu, Y. Long, X. Gao, M. Gao, A. Lei, *Org. Lett.* **2015**, *17*, 2404–2407.

[60] https://echa.europa.eu/it/substance-information/-/substanceinfo/100.028.585.

[61] H. Yi, Z. Liao, G. Zhang, G. Zhang, C. Fan, X. Zhang, E. E. Bunel, C. Pao, J. Lee, A. Lei, *Chem. Eur. J.* **2015**, *21*, 18925–18929.

[62] https://echa.europa.eu/it/substance-information/-/substanceinfo/100.003.395.

[63] R. Matsumoto, H. Nishino, *Synth. Commun.* **2015**, *45*, 1807–1816.

[64] https://echa.europa.eu/it/substance-information/-/substanceinfo/100.000.528.

[65] a) https://www.sigmaaldrich.com/IT/it/sds/mm/1.00263.; b) https://echa.europa.eu/it/substance-information/-/substanceinfo/100.000.527.

[66] J. D. ; A. Tibbetts Hannah E. ;. Cao, Qiao; Grayson, James D. ;. Hobson, Sophie L. ;. Johnson, George D. ;.Turner-Dore, Jacob C. ;. Cresswell, Alexander J., *Synthesis* **2023**, *55*, 3239–3250.

[67] a) X. Zhu, H. Fu, *Chem. Commun.* **2021**, *57*, 9656–9671; b) S. Karmakar, A. Silamkoti, N. A. Meanwell, A. Mathur, A. K. Gupta, *Adv. Synth. Catal.*

2021, *363*, 3693–3736; c) H. L. Chen Yahu A; Liao, Xuebin, *Synthesis* **2020**, *53*, 1–29; d) F. Penteado, E. F. Lopes, D. Alves, G. Perin, R. G. Jacob, E. J. Lenardão, *Chem. Rev.* **2019**, *119*, 7113–7278; e) T. Shao, X. Ban, Z. Jiang, *Chem. Rec.* **2023**, e202300122; f) L. Li, Y. Yao, N. Fu, *Eur. J. Org. Chem.* **2023**, *26*, e202300166.

[68] J. D. Griffin, M. A. Zeller, D. A. Nicewicz, *J. Am. Chem. Soc.* **2015**, *137*, 11340–11348.

[69] J. W. Hilborn, J. A. Pincock, *J. Am. Chem. Soc.* **1991**, *113*, 2683–2686.

[70] D. M. Kitcatt, S. Nicolle, A.-L. Lee, *Chem. Soc. Rev.* **2022**, *51*, 1415–1453.

[71] A. Y. Chan, I. B. Perry, N. B. Bissonnette, B. F. Buksh, G. A. Edwards, L. I. Frye, O. L. Garry, M. N. Lavagnino, B. X. Li, Y. Liang, E. Mao, A. Millet, J. V. Oakley, N. L. Reed, H. A. Sakai, C. P. Seath, D. W. C. MacMillan, *Chem. Rev.* **2022**, *122*, 1485–1542.

[72] a) M. R. Hansen, L. H. Hurley, *Acc. Chem. Res.* **1996**, *29*, 249–258; b) M. Van De Putte, T. Roskams, J. R. Vandenheede, P. Agostinis, P. A. M. De Witte, *Br J Cancer* **2005**, *92*, 1406–1413; c) K. R. Romines, G. A. Freeman, L. T. Schaller, J. R. Cowan, S. S. Gonzales, J. H. Tidwell, C. W. Andrews, D. K. Stammers, R. J. Hazen, R. G. Ferris, S. A. Short, J. H. Chan, L. R. Boone, *J. Med. Chem.* **2006**, *49*, 727–739; d) L. J. Gooßen, F. Rudolphi, C. Oppel, N. Rodríguez, *Angew. Chem. Int. Ed.* **2008**, *47*, 3043–3045.

[73] a) L. J. Gooßen, F. Rudolphi, C. Oppel, N. Rodríguez, *Angew. Chem. Int. Ed.* **2008**, *47*, 3043–3045; b) A. Banerjee, Z. Lei, M.-Y. Ngai, *Synthesis* **2019**, *51*, 303–333; c) E. Voutyritsa, C. G. Kokotos, *Angew Chem Int Ed* **2020**, *59*, 1735–1741; d) L. Li, S. Guo, Q. Wang, J. Zhu, *Org. Lett.* **2019**, *21*, 5462–5466. e) Z. Lei, A. Banerjee, E. Kusevska, E. Rizzo, P. Liu, M. Ngai, *Angew. Chem. Int. Ed.* **2019**, *58*, 7318–7323; f) L. Capaldo, R. Riccardi, D. Ravelli, M. Fagnoni, *ACS Catal.* **2018**, *8*, 304–309; g) P. Fan, C. Zhang, L. Zhang, C. Wang, *Org. Lett.* **2020**, *22*, 3875–3878; h) C. Raviola, S. Protti, D. Ravelli, M. Fagnoni, *Green Chem.* **2019**, *21*, 748–764; i) X. Zhao, B. Li, W. Xia, *Org. Lett.* **2020**, *22*, 1056–1061.

[74] F. Penteado, E. F. Lopes, D. Alves, G. Perin, R. G. Jacob, E. J. Lenardão, *Chem. Rev.* **2019**, *119*, 7113–7278.

[75] A. Rahaman, S. S. Chauhan, S. Bhadra, *Org. Biomol. Chem.* **2023**, *21*, 5691–5724.

[76] a) J. Liu, Q. Liu, H. Yi, C. Qin, R. Bai, X. Qi, Y. Lan, A. Lei, *Angew. Chem. Int. Ed.* **2014**, *53*, 502–506; b) L. Chu, J. M. Lipshultz, D. W. C. MacMillan, *Angew. Chem. Int. Ed.* **2015**, *54*, 7929–7933.

[77] a) C. Zhou, P. Li, X. Zhu, L. Wang, *Org. Lett.* **2015**, *17*, 6198–6201; b) N. Xu, P. Li, Z. Xie, L. Wang, *Chem. Eur. J.* **2016**, *22*, 2236–2242.

[78] https://echa.europa.eu/it/substance-information/-/substanceinfo/100.000.617

[79] D. Payne, *Nature Chem.* **2016**, *8*, 392–392.

[80] B. Su, Z.-C. Cao, Z.-J. Shi, *Acc. Chem. Res.* **2015**, *48*, 886–896.

[81] https://echa.europa.eu/it/substance-information/-/substanceinfo/100.155.819

[82] https://echa.europa.eu/it/substance-information/-/substanceinfo/100.157.643

[83] D.-L. Zhu, Q. Wu, D. J. Young, H. Wang, Z.-G. Ren, H.-X. Li, *Org. Lett.* **2020**, *22*, 6832–6837.

[84] S. Panja, P. Maity, B. C. Ranu, *J. Org. Chem.* **2018**, *83*, 12609–12618.

[85] https://echa.europa.eu/it/substance-information/-/substanceinfo/100.028.897

[86] https://echa.europa.eu/it/substance-information/-/substanceinfo/100.034.608

[87] J. M. Brenan, in *Encyclopedia of Geochemistry: A Comprehensive Reference Source on the Chemistry of the Earth* (Ed.: W.M. White), Springer International Publishing, Cham, **2018**, pp. 1172–1175

[88] L. P. Wu, Y. Suenaga, T. Kuroda-Sowa, M. Maekawa, K. Furuichi, M. Munakata, *Inorganica Chim. Acta* **1996**, *248*, 147–152.

[89] a) M. Johannsen, K. A. Jørgensen, *Chem. Rev.* **1998**, *98*, 1689–1708; b) S. Nag, S. Batra, *Tetrahedron* **2011**, *67*, 8959–9061; c) E. M. Skoda, G. C. Davis, P. Wipf, *Org. Proc. Res. Dev.* **2012**, *16*, 26–34.

[90] a) C. E. Anderson, L. E. Overman, *J. Am. Chem. Soc.* **2003**, *125*, 12412–12413; b) Y. K. Chen, A. E. Lurain, P. J. Walsh, *J. Am. Chem. Soc.* **2002**, *124*, 12225–12231; c) E. Skucas, M.-Y. Ngai, V. Komanduri, M. J. Krische, *Acc. Chem. Res.* **2007**, *40*, 1394–1401; d) N. R. Candeias, F. Montalbano, P. M. S. D. Cal, P. M. P. Gois, *Chem. Rev.* **2010**, *110*, 6169–6193.

[91] A. Noble, D. W. C. MacMillan, *J. Am. Chem. Soc.* **2014**, *136*, 11602–11605

[92] https://echa.europa.eu/it/substance-information/-/substanceinfo/100.004.239

[93] S. Manna, S. Kakumachi, K. K. Das, Y. Tsuchiya, C. Adachi, S. Panda, *Chem. Sci.* **2022**, *13*, 9678–9684.

[94] H. Cao, H. Jiang, H. Feng, J. M. C. Kwan, X. Liu, J. Wu, *J. Am. Chem. Soc.* **2018**, *140*, 16360–16367.

[95] https://echa.europa.eu/it/substance-information/-/substanceinfo/100.003.297

[96] a)https://echa.europa.eu/it/substance-information/-/substanceinfo/100.352.292; b) https://echa.europa.eu/it/substance-information/-/substanceinfo/100.202.643

[97] K. Xu, Z. Tan, H. Zhang, J. Liu, S. Zhang, Z. Wang, *Chem. Commun.* **2017**, *53*, 10719–10722.

[98] https://echa.europa.eu/it/substance-information/-/substanceinfo/100.004.389

[99] R. K. Dieter, C. M. Topping, K. R. Chandupatla, K. Lu, *J. Am. Chem. Soc.* **2001**, *123*, 5132–5133.

[100] https://echa.europa.eu/it/substance-information/-/substanceinfo/100.009.026

[101] https://echa.europa.eu/it/substance-information/-/substanceinfo/100.003.136

[102] https://echa.europa.eu/it/substance-information/-/substanceinfo/100.000.425

[103] https://echa.europa.eu/it/substance-information/-/substanceinfo/100.003.389

[104] https://echa.europa.eu/it/substance-information/-/substanceinfo/100.008.076

[105] S. Reischauer, B. Pieber, *iScience* **2021**, *24*, 102209.